Radiation Dose in Composites

Anthony M. DeStefano
NASA, MSFC, EV44

July 31, 2020

Contents

List of Figures

List of Tables

1 Executive Summary

2 Introduction

3 Material Properties

Basic material properties that are essential in the estimation of dose are material density and thickness. For higher fidelity calculations of dose, the material stoichiometry is required. If a particular material is layered, the material properties of each layer would be needed. Each layer would assumed to be homogeneous in a particular elemental composition.

In Sections 3.1 and 3.2, we discuss assumptions in material properties of composites and multi-layered insulation.

3.1 Composites

To first order, composites are typically composed of a fiber material and a matrix that is dominated by a resin bonding material with additives as a minor component.

3.1.1 Density

In this analysis, three fiber materials were considered:

Table 1: List of approximate fiber densities.

Fiber Type	Density [g cm^{-3}]
Glass	1.9
Aramid	1.4
Carbon	1.6

In composites of interest, the mass percentage of resin is approximately $33 - 35\%$ (e.g., for composite overwrapped pressure vessels (COPVs)). An example density for epoxy resin is about 1.3 g cm^{-3} [*Joven*, 2013]. Therefore, we can approximate the three composite materials as:

Table 2: List of approximate composite densities using fiber densities from Table 1, an epoxy resin density of 1.3 g cm^{-3}, and an epoxy resin mass percentage of $33 - 35\%$.

Composite Type	Density [g cm^{-3}]
Glass + epoxy	1.70
Aramid + epoxy	1.37
Carbon + epoxy	1.50

3.1.2 Thickness

For a given environment, radiation damage to composites is widely dependent on composition, manufacturing processes, size/thickness, and if any shielding is present. In this analysis, a range of thicknesses are considered based on the following components:

Table 3: List of representative materials made of composites with a range of thicknesses.

Composite Component	Min Thickness [mm]	Max Thickness [mm]
COPV	1.5	19
Landing struts	1.5	19
Sandwich panels/Face sheets	0.8	6.5
Solid laminate	1	19

3.1.3 Stoichiometry

At the time of writing, no representative material stoichiometric information has been given. Therefore, placeholder values are assumed that are used in this analysis.

In the SRIM software package, there is a list of common compounds, one of which is epoxy. For the three fiber types shown in Table 1, we assume the most basic elemental composition. Stoichiometry for the epoxy and the fiber materials are shown in Table 4.

Table 4: The epoxy resin composition is taken from the common compound table in SRIM. Glass fiber is assumed to be strictly made of silicon-based glass. The aramid fiber is assumed to be a Nomex or Kevlar type aramid. Carbon fiber is assumed to be made of only carbon.

Material	Stoichiometry [element-count]
Epoxy resin	H-19, C-18, O-3
Glass fiber	O-2, Si-1
Aramid fiber	H-2, C-14, N-2, O-2
Carbon fiber	C-1

If a homogenized substance composed of the epoxy and fiber material is assumed, a net stoichiometry list (see Table 5) can be built using the assumption that the epoxy is $33 - 35\%$ of the total weight of the composite. Densities from Table 2 should be used for each of the composites.

3.1.4 Proton Stopping Distance

The effective stopping (shielding) capabilities for a given proton energy of a composite material can be estimated using SRIM. Using the ion stopping and range table calculator in SRIM, we plug in the stoichiometry (Table 5) and density (Table 2) for each

Table 5: Stoichiometry for each composite is given where the epoxy weight is $33-35\%$ of the total mass.

Material	Stoichiometry [element-count]
Glass composite	H-19, C-18, O-21, Si-9
Aramid composite	H-23, C-46, N-4, O-7
Carbon composite	H-19, C-62, O-3

composite material. The generated output provides the projected range, longitudinal and lateral straggling as a function of ion energy. To estimate the maximum stopping distance of the proton, we take the projected range and add half of the lateral straggling, since we are assuming a normally incident beam. The proton energy range used to generate the stopping distance tables is 10 keV to 1 GeV, completely encompassing the typical energy range of solar energetic particles (SEPs). See Listings 1-4 in Appendix A for the stopping distance tables.

The maximum stopping distance as a function of ion energy can be fit by a double power law given by

$$E[keV] = \frac{a}{\left(\frac{x[mm]}{c}\right)^{-b} + x[mm]^{-d}}, \tag{1}$$

where the ion energy E is in keV and the maximum stopping distance x is in mm. The constant a can be thought of as the largest ion energy (in keV) that roughly 1 mm of material can stop completely. The constant c defines the length scale (in mm) at which low energy ions are affected. The index b is the power law relation that dominates for thin materials (i.e., on the order of c and smaller) and the index d is the power law relation that dominates for thick materials (i.e., much greater than c).

For a given material, keeping the stoichiometry the same, changing the density only changes the constants a and c. If the initial density is ρ_0 and the new density is ρ_1, where $\alpha = \rho_1/\rho_0$, the ion energy is then given by

$$E[keV] = \frac{a\alpha^d}{\left(\frac{x[mm]}{c\alpha^{\frac{d}{b}-1}}\right)^{-b} + x[mm]^{-d}}, \tag{2}$$

where new constants a' and c' can be defined as

$$a' = a\alpha^d, \tag{3}$$

$$c' = c\alpha^{\frac{d}{b}-1}, \tag{4}$$

Fitting Listings 1-4 with Equation 1, the parameters a, b, c, and d are given in Table 6.

In order to compare the stopping distance of equal density materials, we rescale the composites to that of aluminum at 2.702 g cm^{-3} using Equation 2. The rescaled parameters are given in Table 7.

Examining Table 7, for the list of composites in this analysis, the large thickness range (i.e., much greater than c) is independent of material type and density. The

Table 6: Parameters to the double power law fit of the proton energy as a function of maximum stopping distance of composites compared to aluminum of density 2.702 g cm^{-3}.

Material	a [keV]	b	c [mm]	d
Glass composite	1.068E4	1.668	1.31E-2	0.5759
Aramid composite	9.89E3	1.706	1.23E-2	0.5721
Carbon composite	1.039E4	1.699	1.16E-2	0.5717
Aluminum	1.270E4	1.529	1.49E-2	0.5794

Table 7: Parameters to the double power law fit of the proton energy as a function of maximum stopping distance of composites rescaled to the density of aluminum compared to aluminum of density 2.702 g cm^{-3}.

Material	a [keV]	b	c [mm]	d
Glass composite	1.395E4	1.668	9.67E-3	0.5759
Aramid composite	1.46E4	1.706	7.83E-3	0.5721
Carbon composite	1.455E4	1.699	7.85E-3	0.5717
Aluminum	1.270E4	1.529	1.49E-2	0.5794

small-scale range c for the composites is on the order of $8 - 10$ μm and smaller, whereas the small-scale range for aluminum is roughly 15 μm and smaller. The index parameter for small scales b seems to be strongly material dependent, which in turn implies the maximum stopped energy to be strongly dependent on materials for thin materials. Observing the a parameter, the composites tend to have greater stopping capability of protons compared to aluminum. This may have to do with the large number of hydrogen atoms present in the composites themselves, since the collision cross section between hydrogen atoms and protons is higher than large-Z materials.

For larger thicknesses $x \gg c$ (i.e., thicknesses greater than roughly 0.5 mils), we can approximate Equation 1 as

$$E[keV] \sim ax[mm]^d. \tag{5}$$

In order to use the material density to scale the equivalent thickness, a correction factor is needed if data on aluminum is used to estimate stopping power of composites. These scale factors κ can be computed as

$$\kappa_{\text{composite}} = \left(\frac{a_{\text{composite}}}{a_{\text{Al}}} \right)^{1/d}. \tag{6}$$

Therefore, when rescaling the composites to aluminum equivalent thicknesses, the true scaling is given by (taking $d \approx 0.575$)

$$x_{\text{Al equiv}} = \kappa_{\text{composite}} \frac{\rho_{\text{composite}}}{\rho_{\text{Al}}} x_{\text{composite}}, \tag{7}$$

where $x_{\text{composite}}$ is the composite thickness and $x_{\text{Al equiv}}$ is the corrected aluminum

equivalent thickness. The correction factors for the composites studied in this analysis are given in Table 8.

Table 8: Length scale correction factors to aluminum equivalent modeling of composites.

Material	$\kappa_{\text{composite}}$
Glass composite	1.177
Aramid composite	1.272
Carbon composite	1.266

With the correction factors greater than one, an interpretation can be that for a composite and aluminum coupon of similar areal density, more energy will be absorbed (i.e., more ionizing dose) by the composite per areal density since higher energy protons can be stopped in the composite compared to the aluminum equivalent (i.e., the a parameters for the composites are greater than that for aluminum in Table 7). For example, in order to have the same limiting energy as glass composite, the aluminum equivalent thickness must be increased by 17.7%, according to Table 8.

3.2 Multi-layered Insulation (MLI)

Multi-layered insulation, or MLI, is used on spacecraft to aid in thermal management and certain types of radiation and contamination protection. In Chapter 5 of the Spacecraft Thermal Control Handbook [*Donabedian and Gilmore*, 2003], details about MLI applications are descried. Table 9 lists separate components of MLI taken from *Donabedian and Gilmore* [2003].

Table 9: Various components and layers of MLI and their average densities and thicknesses.

Name	Layer	Density [g cm^{-3}]	Thickness [mils]
Beta cloth	outer	1.185	8
Aluminized beta cloth	outer	1.355	8
Kapton	outer	1.50	0.5 - 5
Teflon	outer	2.17	0.5 - 5
Aluminized Kapton	interior	1.50	0.3 - 5
Goldized Kapton	interior	1.50	0.3 - 5
Aluminized mylar	interior	1.38	0.25 - 5
Dacron netting	separator	0.04	6.5
Nomex netting	separator	0.04	6.5
Aluminized polyimide	inner	3.96	0.5 - 3
Double-goldized	inner	5	0.45
Glass-reinforced	inner	5	0.45

Two versions of MLI are constructed to simulate a finite amount of shielding in front of the composite material. In this analysis, aluminized beta cloth - mylar - Nomex is

used which amounts to a density of 1.328 g cm^{-3} and a thickness of 22.5 mils. A thin version of this MLI gives a density of 1.435 g cm^{-3} and a thickness of 5.75 mils. The aluminum equivalent is given in Table 10.

Table 10: Aluminum equivalent thicknesses for placeholder MLIs, assuming an aluminum density of 2.702 g cm^{-3}.

Material	Density g cm^{-3}	Thickness [mils]	Al-equiv thickness [mils,mm]
Thick MLI	1.328	22.5	11.1, 2.81E-1
Thin MLI	1.435	5.75	3.05, 7.76E-2

4 Radiation Environment

The leading radiation environment in interplanetary space is often due to solar energetic particles (SEPs) from solar particle events (SPEs). The geomagnetically unshielded SPE environment is used from SLS-SPEC-159 Design Specification for Natural Environments (DSNE), found in Table 3.3.1.10.2-1, also shown here in Figure 1. The environment is generated using SPENVIS, employing the ESP/PSYCHIC model. The worst case SPE option is used for an override of 1 year with only protons. Output generated from SPENVIS can be found in Listing 5 of Appendix B.

The SPE integral flux can be fit using a Weibull function, given by

$$\Phi(> E[MeV])[\#cm^{-2}] = 9.278 \times 10^{11} \exp\left(-1.821 E^{0.298}\right), \tag{8}$$

or by a double power law,

$$\Phi(> E[MeV])[\#cm^{-2}] = \frac{1.248 \times 10^{11}}{\left(\frac{E}{13.5}\right)^{2.587} + E^{0.6244}}. \tag{9}$$

Shorter time periods than 1 year should not be scaled linearly. Most of the SPE flux is dominated by a few large SPEs, each occurring over at most 1 week.

Other SPE definitions may also be generated directly from the October 1989 SPE, especially for single event effects (SEE). Rates attributed to the peak 5-minute, worst day, and worst week fluxes are often used to define the SPE SEE environment for interplanetary space. Since this analysis is only concerned about TID, a more statistical approach is used, i.e., the ESP/PSYCHIC models.

5 Dose Estimation

Given the limited information available, the total ionizing dose (TID) is estimated in composites. The zeroth order estimation uses the DSNE SPE TID tables, which must assume a finite shielding thickness, shown in Section 5.1. A first order approximation is done by computing dose-depth curves in composites for various energies and incident angles, shown in Section 5.2.

Table 3.3.1.10.2-1. Integral and Differential Proton Fluence of an Unshielded SPE

Proton Energy	Unshielded SPE Integral Fluence per year	Unshielded SPE Differential Fluence per year
MeV	protons/cm²	protons/MeV-cm²
1.00E-01	4.93E+11	2.83E+12
2.50E-01	2.89E+11	6.79E+11
5.00E-01	1.93E+11	2.26E+11
1.00E+00	1.29E+11	7.56E+10
2.00E+00	8.63E+10	2.53E+10
3.50E+00	6.14E+10	1.20E+10
5.00E+00	4.83E+10	7.28E+09
7.10E+00	3.58E+10	4.94E+09
8.00E+00	3.13E+10	4.43E+09
9.00E+00	2.75E+10	3.45E+09
1.00E+01	2.44E+10	2.68E+09
1.60E+01	1.51E+10	9.33E+08
1.80E+01	1.35E+10	7.17E+08
2.00E+01	1.22E+10	6.51E+08
2.50E+01	9.32E+09	4.55E+08
3.50E+01	6.04E+09	2.59E+08
4.00E+01	4.84E+09	2.10E+08
4.50E+01	3.94E+09	1.59E+08
5.00E+01	3.25E+09	1.26E+08
7.10E+01	1.51E+09	5.10E+07
8.00E+01	1.12E+09	3.72E+07
9.00E+01	8.19E+08	2.48E+07
1.00E+02	6.28E+08	1.57E+07
1.60E+02	2.09E+08	3.31E+06
1.80E+02	1.56E+08	2.23E+06
2.00E+02	1.20E+08	1.56E+06
2.50E+02	6.72E+07	7.44E+05
4.00E+02	1.83E+07	1.33E+05
5.00E+02	9.89E+06	4.94E+04

Figure 1: The unshielded SPE integral and differential fluence as defined in DSNE.

Interestingly, using the DSNE tables, the conservative dose estimate assuming at least 3 mils of aluminum shielding is $7.59E4$ rads (which 3 mils of shielding is outside the validity range of SHIELDOSE2, and the dose is in silicon), whereas the dose estimate using SRIM with no shielding in a carbon composite is $6.94E4$ rads. Half of the TID is deposited in the first ~ 15 mils of composite material.

Using Figure 5 it can be concluded that the 3 mils of aluminum shielding absorbed at least 20% of the TID available. This would put the upper-end dose estimate using DNSE with shielding removed to be roughly $9.5E4$ rads.

5.1 DSNE with Shielding

To use the DSNE to estimate dose in composites, a finite shielding layer is forced on the analysis[1]. TID produced by DSNE Table 3.3.1.10.2-1 (Figure 1) can be found in DSNE Table 3.3.1.10.2-3, also shown here in Figure 2.

The principle idea to compute dose in a composite using DSNE is to first compute

[1]The DSNE TID tables in concern were developed using SHEILDOSE2, which implicitly assumes a finite range of shielding thicknesses.

Table 3.3.1.10.2-3. Total Unshielded SPE TID Inside Al Shielding

Aluminum Shield Depth	Total SPE TID
mm	cGy(Si)/year
1.00E-02	3.41E+05
2.50E-02	1.69E+05
5.00E-02	1.03E+05
1.00E-01	6.43E+04
2.00E-01	4.01E+04
3.00E-01	3.00E+04
4.00E-01	2.33E+04
5.00E-01	1.84E+04
6.00E-01	1.50E+04
8.00E-01	1.11E+04
1.00E+00	8.83E+03
2.50E+00	3.91E+03
5.00E+00	1.97E+03
1.00E+01	8.87E+02
1.20E+01	7.03E+02
1.40E+01	5.57E+02
1.60E+01	4.53E+02
1.80E+01	3.77E+02
2.00E+01	3.18E+02
3.00E+01	1.50E+02
5.00E+01	5.97E+01
7.50E+01	2.94E+01
1.00E+02	1.73E+01

Figure 2: The TID in silicon as a function of aluminum shielding from unshielded SPE fluence as defined in DSNE.

the dose with only a thin amount of shielding. In this analysis, two thicknesses of MLI have been considered (11.1 and 3.05 mils of aluminum equivalent thickness), shown in Table 10. Dose in silicon after this MLI shielding is denoted by D_{MLI}. The next step is to add the thickness of the MLI layer and the composite layer (Table 3, spanning 31.5 to 748 mils of composite) as a single layer of aluminum equivalent thickness and compute the dose, $D_{\text{MLI+Composite}}$. The dose in only the composite is then computed by the difference between these two doses,

$$D_{\text{composite}} = D_{\text{MLI}} - D_{\text{MLI+Composite}}. \tag{10}$$

To compute a dose D_{layer} from DSNE Table 3.3.1.10.2-3 (Figure 2), a power law interpolation scheme can be used to estimate dose for a shielding thickness x_{layer} between two rows in the table. The interpolation scheme for the layer dose is given by

$$D_{\text{layer}} = D_i \left(\frac{D_{i+1}}{D_i} \right)^{\frac{\log(x_{\text{layer}}/x_i)}{\log(x_{i+1}/x_i)}}, \tag{11}$$

where $x_{i+1} \geqslant x_{\text{layer}} > x_i$, for x in units of mm and D in units of cGy(Si) per year.

Examining Table 11, the range of doses is from $2.023E4$ rad to $7.594E4$ rad. Any finite amount of shielding can limit the dose to the composite layer. The doses estimated using the thin MLI case are just above the minimum limit of 0.05 mm (or 2 mils)

Table 11: Estimation of dose using DSNE Table 3.3.1.10.2-3 in composites with two MLI shielding thicknesses and three composites each with two thicknesses (31.5 mils and 748 mils of composite). Thicknesses of MLI and composites were converted to aluminum equivalent thicknesses. The correction factor for each composite (Table 8) is used to derive the aluminum equivalent thickness.

	Thin MLI (3.05 mils Al)	Thick MLI (11.1 mils Al)
Composite	TID dose [rad]	TID dose [rad]
Thin glass (23.3 mils Al)	6.312E4	2.123E4
Thick glass (554 mils Al)	7.594E4	3.083E4
Thin aramid (20.3 mils Al)	6.130E4	2.023E4
Thick aramid (482 mils Al)	7.581E4	3.070E4
Thin carbon (22.1 mils Al)	6.246E4	2.086E4
Thick carbon (526 mils Al)	7.589E4	3.078E4

that SHIELDOSE2 can handle[2,3]. It is expected that by removing the MLI shielding, the estimated doses will be greater (by at least 25%) than the $7.594E4$ rad upper limit shown in Table 11. However, further analysis is required to sharpen this dose estimate in composites. In Section 5.2, dose estimates in higher fidelity composite surrogates using SRIM with no shielding is discussed.

5.2 SRIM without Shielding

The Stopping and Range of Ions in Matter (SRIM) [*Ziegler et al.*, 2009] is a group of programs that calculate the stopping and range of ions in matter[4]. The ion stopping and range table calculator in SRIM was used in Section 3.1.4. For each run using TRIM (Transport of Ions in Matter), a mono-energetic beam of a single incident angle is used at the environment and transported through a series of predefined layers in a Monte Carlo fashion.

The isotropic flux for a particular energy and incident angle $\Phi(E,\theta)$ can be computed as (using a cosine distribution for an incident isotropic distribution on a flat slab)

$$\Phi(E,\theta) = [\Phi(E_i) - \Phi(E_{i+1})]\frac{\cos(2\theta_i) - \cos(2\theta_{i+1})}{2}, \tag{12}$$

where $E = \sqrt{E_i E_{i+1}}$, $\theta = (\theta_i + \theta_{i+1})/2$, and $\Phi(E_i)$ is the integral flux at energy E_i (e.g., DSNE Table 3.3.1.10.2-1, or Figure 1). The TRIM simulation is ran using E and θ as centered values in the energy-angle bin. The anglular weight term follows from the integral

$$w_i = 2\int_{\theta_i}^{\theta_{i+1}} d\theta \sin\theta\cos\theta = \frac{\cos(2\theta_i) - \cos(2\theta_{i+1})}{2}, \tag{13}$$

[2] https://www.spenvis.oma.be/help/background/shieldose/shieldose.html
[3] https://www.spenvis.oma.be/help/models/sd2q.html
[4] http://www.srim.org/SRIM/SRIMINTRO.htm

were it is assumed that the incident angle θ ranges[5] from 0° to 90°, hence the factor of 2. In this analysis, the range of incident angles θ are given in Table 12.

Table 12: Angular weight factors w_i where $\sum_i w_i = 1$. The θ_i and θ_{i+1} are bin edges where θ is taken as the approximate bin center.

index i	θ_i	θ_{i+1}	θ	w_i
0	0.00	15.0	0.00	3.40E-2
1	15.0	37.5	30.0	1.73E-1
2	37.5	52.5	45.0	1.85E-1
3	52.5	67.5	60.0	2.26E-1
4	67.5	82.5	75.0	2.52E-1
5	82.5	90.0	87.0	1.30E-1

TID can be computed by saving the ionization file once a sufficient number of test particles are ran. The ionization file contains information about the deposited ionization energy due to the primary ions D_{ions} and to secondaries D_{recoils} (called recoils) as a function of target depth. The ionization energy units are in eV per Angstrom per ion. To convert the deposited energy into rads, as a function of incident ion energy, angle and deposited depth, the following conversion equation is used

$$D(E,\theta,r) = [D_{\text{ions}} + D_{\text{recoils}}](r) \times \frac{10^8 \text{ Å}}{\text{cm}} \times \frac{1.60218 \times 10^{-19} \text{ J}}{\text{eV}} \times \frac{\Phi(E,\theta)}{\rho[\text{kg cm}^{-3}]}, \quad (14)$$

where ρ is the material density in units of kg cm^{-3}. The dose as a function of energy or as a function of depth (see Figure 3) can be calculated by summing over the other variables.

The dose-depth profile in a carbon composite is shown in Figure 3 for a composite thickness of 20 mm. Artifacts can be seen at larger depth since a finite number of energies were probed. The spikes are due to individual Bragg peaks. With a greater number of energies probed, these spikes would be smoothed out.

Another way to look at the dose profile is total dose as a function of thickness, shown in Figure 4.

The dose as a function of ion energy is given in Figure 5, which is independent of geometry type, slab or sphere. In Section 5.1, the thinnest shielding assumed was 7.76×10^{-2} mm of aluminum equivalent. Using Table 6, energies less than 2.8 MeV would be completely absorbed in the aluminum shielding. Therefore, using Figure 5 it can be concluded that the thin shielding absorbed at least 20% of the TID available. This would put the upper-end dose estimate using DNSE to be roughly $9.5E4$ rads.

In order to compare total doses computed in SRIM with the DSNE dose estimates done in Section 5.1, the slab doses must be converted to doses in a sphere. Equation (9) of *Seltzer* [1986] enables the determination of doses in a sphere, which is given by

$$D_{\text{sphere}}(0,r) = 2\left[D_{\text{slab}}(r) - r\frac{dD_{\text{slab}}(r)}{dr}\right]. \quad (15)$$

[5] Initially, the range of the incident angle is from -90° to 90°, but it is assumed the dose profiles will be symmetric about 0°.

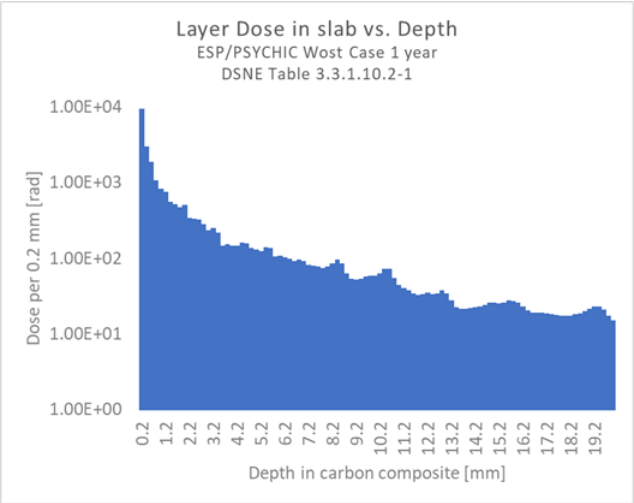

Figure 3: Dose per 0.2 mm as a function of depth in a slab using DSNE Table 3.3.1.10.2-1 as the ion environment.

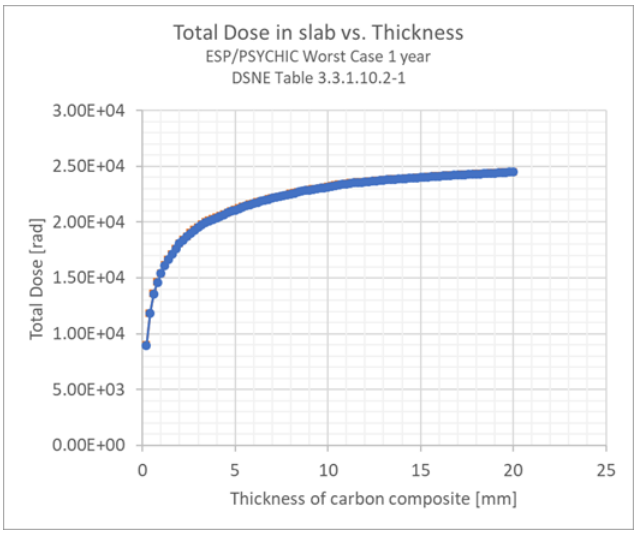

Figure 4: Total dose as a function of carbon composite thickness in a slab using DSNE Table 3.3.1.10.2-1 as the ion environment.

To better approximate the derivative term, a power law interpolation fit can be made between each dose-depth pair. The dose in a slab can be approximated as

$$D_{\text{slab}}(r) \approx D_i \left(\frac{D_{i+1}}{D_i} \right)^{\frac{\log(r/r_i)}{\log(r_{i+1}/r_i)}} , \tag{16}$$

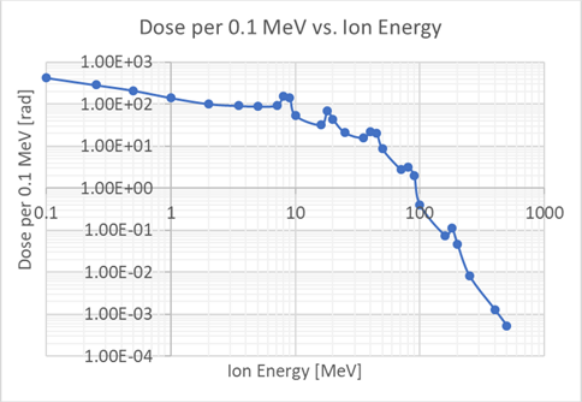

Figure 5: Dose per 0.1 MeV as a function of ion energy using DSNE Table 3.3.1.10.2-1 as the ion environment.

where $r_{i+1} \geqslant r \geqslant r_i$ and the D_i's are the doses at depth r_i. Taking the derivative of Equation (16),

$$\frac{dD_{\text{slab}}(r)}{dr} = \frac{\log\left(\frac{D_{i+1}}{D_i}\right)}{\log\left(\frac{r_{i+1}}{r_i}\right)} \frac{D_{\text{slab}}(r)}{r}, \tag{17}$$

and plugging into Equation (15), the dose at the center of a sphere of radius r now reads

$$D_{\text{sphere}}(0, r) \approx 2D_{\text{slab}}(r) \left[1 - \frac{\log\left(\frac{D_{i+1}}{D_i}\right)}{\log\left(\frac{r_{i+1}}{r_i}\right)}\right]. \tag{18}$$

To better approximate the derivative term (which is used in this analysis), r can be taken to be r_{i+1} and use both the left and right sided approximation (this works if $i \neq 0$ or $i + 1 \neq N - 1$, where N is the total number of depths) so that the dose in a sphere can be written as

$$D_{\text{sphere}}(0, r_{i+1}) \approx 2D_{\text{slab}}(r_{i+1}) \left[1 - \frac{\log\left(\frac{D_{i+1}}{D_i}\right) / \log\left(\frac{r_{i+1}}{r_i}\right) + \log\left(\frac{D_{i+2}}{D_{i+1}}\right) / \log\left(\frac{r_{i+2}}{r_{i+1}}\right)}{2}\right]. \tag{19}$$

After resampling the depth bins to a lower resolution to avoid the artifact jumps (which would mess up the derivative term), Figures 3 and 4 are converted to doses in a sphere, shown in Figures 6 and 7, respectively.

From Figure 7, the TID absorbed by 20 mm of carbon composite is 6.94×10^4 rads. Half of this total dose is absorbed in the first 0.4 mm or 15 mils of the carbon composite, and 75% of the total dose is absorbed in the first 2.5 mm or 100 mils of carbon composite.

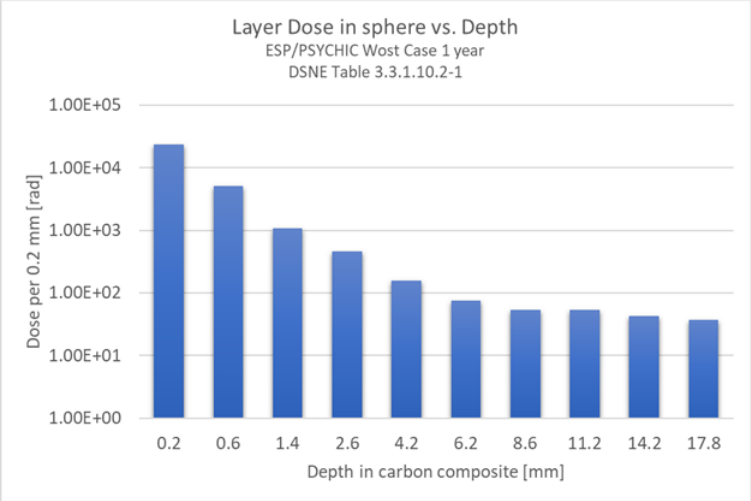

Figure 6: Dose per 0.2 mm as a function of depth in a sphere using DSNE Table 3.3.1.10.2-1 as the ion environment.

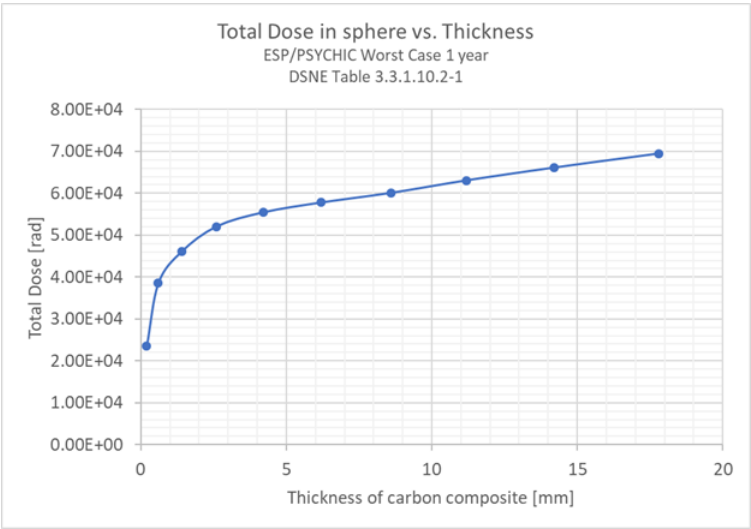

Figure 7: Total dose as a function of carbon composite thickness in a sphere using DSNE Table 3.3.1.10.2-1 as the ion environment.

6 SRIM Comparison with DSNE (SHIELDOSE2)

The doses computed in SRIM are compared with DSNE Table 3.3.1.10.2-3 (see Figure 2). First, the SRIM doses are computed in a slab using the SPE worst case 1 year environment (DSNE Table 3.3.1.10.2-1) and are compared with doses computed in

SPENVIS. The same exact set of knobs is used in computing DSNE Table 3.3.1.10.2-3, except the slab option is used instead. It doesn't matter whether a finite or infinite slab is used. Both were checked and there were no differences with this particular energy spectrum and ion (protons). The SRIM doses in a slab and sphere are summarized in Table 13 and comparisons with SHIELDOSE2 (see Appendix B) are shown in Figure 8.

Table 13: Dose to silicon in slab and spherical geometric as a function of aluminum shielding thickness. Equation (19) was used to convert slab doses to sphere doses.

Al thickness [mm]	Dose in slab [rad]	Dose in sphere [rad]
1.0E-2	1.57E5	5.45E5
1.0E-1	3.31E4	1.15E5
1.0E+0	3.52E3	1.29E4
1.0E+1	2.73E2	1.07E3
1.0E+2	4.54E0	2.63E1

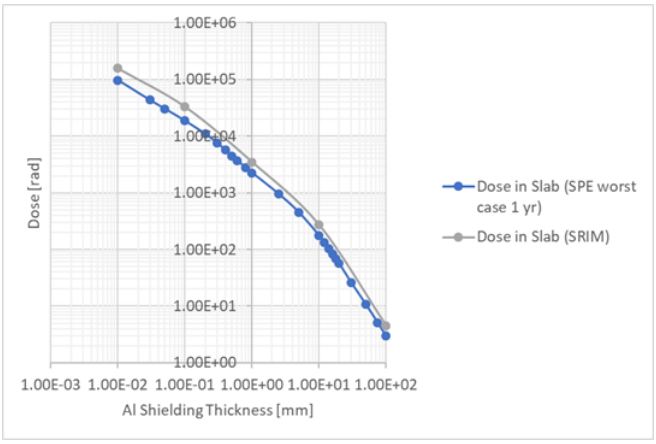

Figure 8: Comparison between slab dose as a function of aluminum shielding thickness of SRIM and SPENVIS (i.e., SHIELDOSE2) runs.

The doses computed in SRIM are consistently overestimated compared with SHIELDOSE2, which is a consequence of low-resolution sampling of the energy-angle space of the incident ion spectrum. In this analysis, only normally incident ions were considered. One calculation was done with a shielding thickness of 1 mm that took into account additional angular information of the isotropic spectrum. The estimated dose in silicon of spherical geometry turned out to be 8.55×10^3 rads whereas the DSNE value is 8.83×10^3 rads. This shows that better angular resolution could lower the SRIM dose estimates shown in Figure 8.

The SRIM-DSNE comparison shown in Figure 9 is in much better agreement, which is a way of validation of SRIM for the analysis given in Section 5.2.

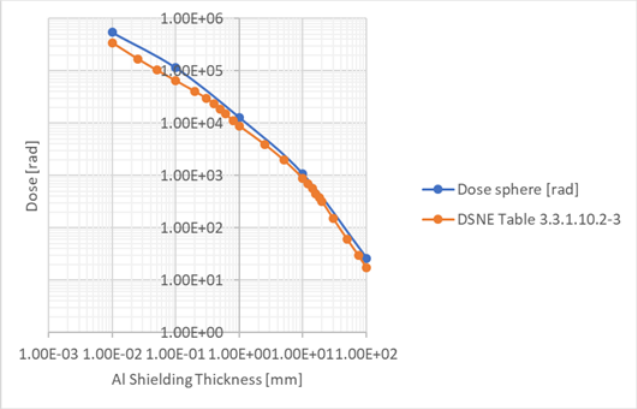

Figure 9: Comparison between sphere dose as a function of aluminum shielding thickness of SRIM and SPENVIS (i.e., SHIELDOSE2) runs.

A Ion Stopping and Range Tables

Listing 1: Ion stopping and range tables of protons in glass composite.

```
 1  ==================================================================
 2              SRIM version  ---> SRIM-2013.00
 3              Calc. date    ---> July 29, 2020
 4  ==================================================================
 5
 6  Disk File Name = SRIM Outputs\Hydrogen in Glass Composite.txt
 7
 8  Ion = Hydrogen [1] , Mass = 1.008 amu
 9
10  Target Density =  1.7000E+00 g/cm3 = 8.3236E+22 atoms/cm3
11  ======= Target  Composition ========
12     Atom    Atom    Atomic     Mass
13     Name    Numb    Percent    Percent
14     ____    ____    _______    _______
15       H       1     028.36     002.32
16       C       6     026.87     026.24
17       O       8     031.34     040.77
18      Si      14     013.43     030.67
19  ====================================
20  Bragg Correction = -3.61%
21  Stopping Units =  MeV / (mg/cm2)
22  See bottom of Table for other Stopping units
23
24          Ion          dE/dx        dE/dx      Projected   Longitudinal    Lateral
25       Energy          Elec.        Nuclear      Range      Straggling    Straggling
26  ____________    _________    _________    ___________    ___________    ___________
27   10.00 keV      3.417E-01    5.866E-03     1809 A         578 A          572 A
28   11.00 keV      3.573E-01    5.508E-03     1952 A         597 A          598 A
29   12.00 keV      3.721E-01    5.197E-03     2092 A         614 A          622 A
30   13.00 keV      3.863E-01    4.924E-03     2227 A         629 A          645 A
```

14.00	keV	3.998E−01	4.681E−03	2359	A	643 A	666 A
15.00	keV	4.126E−01	4.464E−03	2488	A	656 A	685 A
16.00	keV	4.249E−01	4.269E−03	2614	A	668 A	704 A
17.00	keV	4.365E−01	4.092E−03	2737	A	679 A	721 A
18.00	keV	4.476E−01	3.931E−03	2858	A	690 A	738 A
20.00	keV	4.683E−01	3.648E−03	3093	A	709 A	768 A
22.50	keV	4.914E−01	3.352E−03	3375	A	731 A	803 A
25.00	keV	5.119E−01	3.106E−03	3648	A	749 A	835 A
27.50	keV	5.301E−01	2.897E−03	3913	A	766 A	864 A
30.00	keV	5.462E−01	2.717E−03	4170	A	781 A	890 A
32.50	keV	5.605E−01	2.560E−03	4422	A	795 A	915 A
35.00	keV	5.732E−01	2.422E−03	4668	A	808 A	938 A
37.50	keV	5.844E−01	2.300E−03	4911	A	820 A	960 A
40.00	keV	5.944E−01	2.190E−03	5150	A	831 A	981 A
45.00	keV	6.110E−01	2.003E−03	5618	A	852 A	1020 A
50.00	keV	6.238E−01	1.848E−03	6078	A	871 A	1056 A
55.00	keV	6.334E−01	1.717E−03	6531	A	888 A	1089 A
60.00	keV	6.403E−01	1.605E−03	6980	A	904 A	1121 A
65.00	keV	6.449E−01	1.508E−03	7425	A	920 A	1150 A
70.00	keV	6.475E−01	1.423E−03	7869	A	934 A	1179 A
80.00	keV	6.480E−01	1.281E−03	8757	A	965 A	1233 A
90.00	keV	6.436E−01	1.166E−03	9650	A	994 A	1285 A
100.00	keV	6.357E−01	1.072E−03	1.06	um	1021 A	1334 A
110.00	keV	6.254E−01	9.934E−04	1.15	um	1048 A	1383 A
120.00	keV	6.136E−01	9.262E−04	1.24	um	1074 A	1430 A
130.00	keV	6.008E−01	8.682E−04	1.34	um	1101 A	1477 A
140.00	keV	5.875E−01	8.175E−04	1.43	um	1127 A	1525 A
150.00	keV	5.741E−01	7.729E−04	1.53	um	1153 A	1572 A
160.00	keV	5.607E−01	7.332E−04	1.64	um	1179 A	1620 A
170.00	keV	5.476E−01	6.978E−04	1.74	um	1205 A	1668 A
180.00	keV	5.348E−01	6.658E−04	1.85	um	1232 A	1716 A
200.00	keV	5.104E−01	6.105E−04	2.07	um	1306 A	1815 A
225.00	keV	4.826E−01	5.539E−04	2.37	um	1413 A	1944 A
250.00	keV	4.576E−01	5.076E−04	2.68	um	1522 A	2078 A
275.00	keV	4.353E−01	4.689E−04	3.00	um	1634 A	2218 A
300.00	keV	4.153E−01	4.360E−04	3.35	um	1749 A	2364 A
325.00	keV	3.973E−01	4.078E−04	3.71	um	1867 A	2516 A
350.00	keV	3.811E−01	3.832E−04	4.08	um	1988 A	2675 A
375.00	keV	3.665E−01	3.616E−04	4.47	um	2112 A	2839 A
400.00	keV	3.532E−01	3.424E−04	4.88	um	2238 A	3010 A
450.00	keV	3.298E−01	3.100E−04	5.73	um	2638 A	3369 A
500.00	keV	3.100E−01	2.835E−04	6.65	um	3033 A	3750 A
550.00	keV	2.930E−01	2.614E−04	7.62	um	3426 A	4154 A
600.00	keV	2.782E−01	2.428E−04	8.64	um	3820 A	4577 A
650.00	keV	2.653E−01	2.267E−04	9.72	um	4215 A	5021 A
700.00	keV	2.538E−01	2.128E−04	10.85	um	4613 A	5483 A
800.00	keV	2.345E−01	1.898E−04	13.25	um	5919 A	6461 A
900.00	keV	2.188E−01	1.715E−04	15.83	um	7151 A	7503 A
1.00	MeV	2.060E−01	1.566E−04	18.59	um	8345 A	8604 A
1.10	MeV	1.971E−01	1.442E−04	21.50	um	9507 A	9752 A
1.20	MeV	1.883E−01	1.337E−04	24.54	um	1.06 um	1.09 um
1.30	MeV	1.795E−01	1.248E−04	27.73	um	1.18 um	1.22 um
1.40	MeV	1.716E−01	1.170E−04	31.06	um	1.29 um	1.34 um
1.50	MeV	1.644E−01	1.102E−04	34.55	um	1.41 um	1.48 um
1.60	MeV	1.578E−01	1.041E−04	38.19	um	1.52 um	1.61 um
1.70	MeV	1.517E−01	9.876E−05	41.98	um	1.64 um	1.75 um
1.80	MeV	1.460E−01	9.395E−05	45.92	um	1.76 um	1.90 um

88	2.00 MeV	1.357E−01	8.568E−05	54.25 um	2.16 um	2.21 um
89	2.25 MeV	1.249E−01	7.728E−05	65.51 um	2.75 um	2.61 um
90	2.50 MeV	1.157E−01	7.045E−05	77.70 um	3.30 um	3.05 um
91	2.75 MeV	1.079E−01	6.478E−05	90.83 um	3.85 um	3.52 um
92	3.00 MeV	1.011E−01	6.000E−05	104.86 um	4.40 um	4.01 um
93	3.25 MeV	9.527E−02	5.591E−05	119.80 um	4.96 um	4.54 um
94	3.50 MeV	9.012E−02	5.236E−05	135.62 um	5.51 um	5.09 um
95	3.75 MeV	8.555E−02	4.926E−05	152.32 um	6.08 um	5.67 um
96	4.00 MeV	8.146E−02	4.653E−05	169.89 um	6.65 um	6.27 um
97	4.50 MeV	7.447E−02	4.191E−05	207.55 um	8.68 um	7.57 um
98	5.00 MeV	6.869E−02	3.817E−05	248.56 um	10.60 um	8.96 um
99	5.50 MeV	6.382E−02	3.507E−05	292.86 um	12.49 um	10.47 um
100	6.00 MeV	5.966E−02	3.245E−05	340.40 um	14.37 um	12.07 um
101	6.50 MeV	5.605E−02	3.022E−05	391.13 um	16.26 um	13.77 um
102	7.00 MeV	5.290E−02	2.829E−05	445.00 um	18.17 um	15.57 um
103	8.00 MeV	4.764E−02	2.510E−05	561.90 um	24.95 um	19.45 um
104	9.00 MeV	4.341E−02	2.259E−05	690.95 um	31.32 um	23.71 um
105	10.00 MeV	3.993E−02	2.056E−05	831.91 um	37.57 um	28.33 um
106	11.00 MeV	3.702E−02	1.887E−05	984.55 um	43.81 um	33.31 um
107	12.00 MeV	3.454E−02	1.745E−05	1.15 mm	50.10 um	38.64 um
108	13.00 MeV	3.240E−02	1.624E−05	1.32 mm	56.47 um	44.31 um
109	14.00 MeV	3.053E−02	1.519E−05	1.51 mm	62.94 um	50.32 um
110	15.00 MeV	2.889E−02	1.428E−05	1.71 mm	69.52 um	56.66 um
111	16.00 MeV	2.743E−02	1.347E−05	1.92 mm	76.21 um	63.33 um
112	17.00 MeV	2.612E−02	1.275E−05	2.14 mm	83.02 um	70.32 um
113	18.00 MeV	2.495E−02	1.211E−05	2.37 mm	89.96 um	77.63 um
114	20.00 MeV	2.292E−02	1.101E−05	2.86 mm	115.11 um	93.19 um
115	22.50 MeV	2.085E−02	9.900E−06	3.53 mm	151.04 um	114.37 um
116	25.00 MeV	1.915E−02	8.999E−06	4.26 mm	185.25 um	137.40 um
117	27.50 MeV	1.774E−02	8.255E−06	5.06 mm	218.88 um	162.25 um
118	30.00 MeV	1.654E−02	7.628E−06	5.92 mm	252.44 um	188.88 um
119	32.50 MeV	1.551E−02	7.094E−06	6.83 mm	286.21 um	217.22 um
120	35.00 MeV	1.462E−02	6.632E−06	7.81 mm	320.31 um	247.26 um
121	37.50 MeV	1.383E−02	6.228E−06	8.84 mm	354.84 um	278.96 um
122	40.00 MeV	1.314E−02	5.873E−06	9.93 mm	389.84 um	312.28 um
123	45.00 MeV	1.197E−02	5.276E−06	12.27 mm	517.07 um	383.67 um
124	50.00 MeV	1.101E−02	4.793E−06	14.83 mm	636.98 um	461.20 um
125	55.00 MeV	1.021E−02	4.394E−06	17.59 mm	754.06 um	544.65 um
126	60.00 MeV	9.541E−03	4.058E−06	20.57 mm	870.29 um	633.81 um
127	65.00 MeV	8.965E−03	3.772E−06	23.74 mm	986.65 um	728.50 um
128	70.00 MeV	8.466E−03	3.525E−06	27.11 mm	1.10 mm	828.55 um
129	80.00 MeV	7.644E−03	3.120E−06	34.41 mm	1.53 mm	1.04 mm
130	90.00 MeV	6.993E−03	2.801E−06	42.44 mm	1.92 mm	1.28 mm
131	100.00 MeV	6.465E−03	2.543E−06	51.18 mm	2.30 mm	1.53 mm
132	110.00 MeV	6.028E−03	2.330E−06	60.58 mm	2.67 mm	1.80 mm
133	120.00 MeV	5.659E−03	2.151E−06	70.64 mm	3.05 mm	2.09 mm
134	130.00 MeV	5.344E−03	1.999E−06	81.31 mm	3.42 mm	2.39 mm
135	140.00 MeV	5.073E−03	1.867E−06	92.59 mm	3.80 mm	2.71 mm
136	150.00 MeV	4.835E−03	1.752E−06	104.45 mm	4.17 mm	3.05 mm
137	160.00 MeV	4.626E−03	1.651E−06	116.87 mm	4.55 mm	3.39 mm
138	170.00 MeV	4.441E−03	1.562E−06	129.82 mm	4.94 mm	3.75 mm
139	180.00 MeV	4.275E−03	1.482E−06	143.30 mm	5.32 mm	4.12 mm
140	200.00 MeV	3.992E−03	1.345E−06	171.74 mm	6.72 mm	4.90 mm
141	225.00 MeV	3.706E−03	1.206E−06	209.92 mm	8.68 mm	5.92 mm
142	250.00 MeV	3.476E−03	1.095E−06	250.83 mm	10.50 mm	7.01 mm
143	275.00 MeV	3.287E−03	1.002E−06	294.27 mm	12.23 mm	8.15 mm
144	300.00 MeV	3.130E−03	9.250E−07	340.05 mm	13.91 mm	9.33 mm

```
325.00 MeV   2.996E-03  8.591E-07  388.01 mm    15.55 mm    10.55 mm
350.00 MeV   2.881E-03  8.022E-07  437.99 mm    17.16 mm    11.81 mm
375.00 MeV   2.782E-03  7.526E-07  489.86 mm    18.74 mm    13.10 mm
400.00 MeV   2.696E-03  7.090E-07  543.48 mm    20.30 mm    14.42 mm
450.00 MeV   2.552E-03  6.357E-07  655.48 mm    25.90 mm    17.13 mm
500.00 MeV   2.438E-03  5.766E-07  773.25 mm    30.94 mm    19.91 mm
550.00 MeV   2.346E-03  5.278E-07  896.07 mm    35.63 mm    22.75 mm
600.00 MeV   2.271E-03  4.869E-07    1.02 m     40.07 mm    25.63 mm
650.00 MeV   2.208E-03  4.521E-07    1.15 m     44.31 mm    28.54 mm
700.00 MeV   2.155E-03  4.220E-07    1.29 m     48.39 mm    31.47 mm
800.00 MeV   2.071E-03  3.728E-07    1.57 m     62.63 mm    37.35 mm
900.00 MeV   2.009E-03  3.341E-07    1.86 m     74.98 mm    43.23 mm
  1.00 GeV   1.962E-03  3.029E-07    2.15 m     86.12 mm    49.06 mm

 Multiply Stopping by        for Stopping Units
 -------------------        ------------------

  1.6999E+01                 eV / Angstrom
  1.6999E+02                keV / micron
  1.6999E+02                MeV / mm
  1.0000E+00                keV / (ug/cm2)
  1.0000E+00                MeV / (mg/cm2)
  1.0000E+03                keV / (mg/cm2)
  2.0423E+01                 eV / (1E15 atoms/cm2)
  1.0643E+01                L.S.S. reduced units
 ================================================================
 (C) 1984,1989,1992,1998,2008 by J.P. Biersack and J.F. Ziegler
```

Listing 2: Ion stopping and range tables of protons in aramid composite.

```
 ================================================================
              SRIM version ---> SRIM-2013.00
              Calc. date   ---> July 29, 2020
 ================================================================

 Disk File Name = SRIM Outputs\Hydrogen in Aramid Composite.txt

 Ion = Hydrogen [1] , Mass = 1.008 amu

 Target Density =  1.3700E+00 g/cm3 = 8.8746E+22 atoms/cm3
 ======= Target  Composition ========
    Atom    Atom    Atomic     Mass
    Name    Numb    Percent    Percent
    ----    ----    -------    -------
      H       1     028.75     003.12
      C       6     057.50     074.29
      O       8     008.75     015.06
      N       7     005.00     007.53
 ====================================
 Bragg Correction = -3.61%
 Stopping Units =  MeV / (mg/cm2)
 See bottom of Table for other Stopping units

        Ion          dE/dx       dE/dx      Projected   Longitudinal    Lateral
      Energy         Elec.       Nuclear      Range      Straggling    Straggling
 ------------------ ---------- ---------- ------------ ------------ ------------
  10.00 keV   4.205E-01  6.757E-03    1987 A       524 A        545 A
  11.00 keV   4.388E-01  6.327E-03    2139 A       538 A        567 A
```

29	12.00 keV	4.560E−01	5.955E−03	2286 A	552 A	588 A
30	13.00 keV	4.721E−01	5.628E−03	2429 A	564 A	607 A
31	14.00 keV	4.874E−01	5.340E−03	2568 A	575 A	625 A
32	15.00 keV	5.017E−01	5.083E−03	2704 A	585 A	641 A
33	16.00 keV	5.154E−01	4.852E−03	2837 A	594 A	657 A
34	17.00 keV	5.283E−01	4.644E−03	2967 A	602 A	672 A
35	18.00 keV	5.405E−01	4.454E−03	3094 A	611 A	686 A
36	20.00 keV	5.631E−01	4.123E−03	3343 A	626 A	712 A
37	22.50 keV	5.885E−01	3.779E−03	3642 A	642 A	742 A
38	25.00 keV	6.109E−01	3.492E−03	3932 A	657 A	768 A
39	27.50 keV	6.309E−01	3.251E−03	4213 A	670 A	793 A
40	30.00 keV	6.487E−01	3.043E−03	4487 A	682 A	815 A
41	32.50 keV	6.646E−01	2.863E−03	4754 A	693 A	836 A
42	35.00 keV	6.789E−01	2.705E−03	5017 A	703 A	856 A
43	37.50 keV	6.918E−01	2.565E−03	5274 A	712 A	874 A
44	40.00 keV	7.033E−01	2.440E−03	5528 A	721 A	892 A
45	45.00 keV	7.229E−01	2.226E−03	6026 A	738 A	924 A
46	50.00 keV	7.384E−01	2.049E−03	6514 A	754 A	954 A
47	55.00 keV	7.504E−01	1.901E−03	6994 A	769 A	982 A
48	60.00 keV	7.594E−01	1.775E−03	7468 A	782 A	1008 A
49	65.00 keV	7.656E−01	1.665E−03	7938 A	795 A	1033 A
50	70.00 keV	7.694E−01	1.569E−03	8405 A	806 A	1056 A
51	80.00 keV	7.710E−01	1.410E−03	9339 A	834 A	1101 A
52	90.00 keV	7.662E−01	1.282E−03	1.03 um	860 A	1143 A
53	100.00 keV	7.567E−01	1.177E−03	1.12 um	884 A	1183 A
54	110.00 keV	7.440E−01	1.089E−03	1.22 um	909 A	1223 A
55	120.00 keV	7.291E−01	1.014E−03	1.32 um	932 A	1261 A
56	130.00 keV	7.130E−01	9.496E−04	1.42 um	956 A	1300 A
57	140.00 keV	6.962E−01	8.934E−04	1.52 um	980 A	1338 A
58	150.00 keV	6.792E−01	8.440E−04	1.62 um	1004 A	1377 A
59	160.00 keV	6.624E−01	8.001E−04	1.73 um	1029 A	1415 A
60	170.00 keV	6.458E−01	7.608E−04	1.84 um	1053 A	1454 A
61	180.00 keV	6.298E−01	7.255E−04	1.96 um	1078 A	1494 A
62	200.00 keV	5.993E−01	6.645E−04	2.19 um	1154 A	1575 A
63	225.00 keV	5.647E−01	6.022E−04	2.51 um	1267 A	1681 A
64	250.00 keV	5.339E−01	5.512E−04	2.84 um	1382 A	1792 A
65	275.00 keV	5.064E−01	5.087E−04	3.19 um	1499 A	1908 A
66	300.00 keV	4.820E−01	4.727E−04	3.55 um	1620 A	2029 A
67	325.00 keV	4.601E−01	4.417E−04	3.94 um	1743 A	2157 A
68	350.00 keV	4.404E−01	4.148E−04	4.34 um	1868 A	2290 A
69	375.00 keV	4.226E−01	3.912E−04	4.76 um	1996 A	2429 A
70	400.00 keV	4.065E−01	3.702E−04	5.20 um	2126 A	2573 A
71	450.00 keV	3.784E−01	3.348E−04	6.13 um	2566 A	2878 A
72	500.00 keV	3.546E−01	3.060E−04	7.12 um	2993 A	3205 A
73	550.00 keV	3.343E−01	2.819E−04	8.18 um	3415 A	3551 A
74	600.00 keV	3.166E−01	2.616E−04	9.30 um	3835 A	3918 A
75	650.00 keV	3.012E−01	2.442E−04	10.47 um	4255 A	4302 A
76	700.00 keV	2.875E−01	2.290E−04	11.71 um	4677 A	4704 A
77	800.00 keV	2.646E−01	2.041E−04	14.35 um	6121 A	5559 A
78	900.00 keV	2.460E−01	1.842E−04	17.20 um	7470 A	6475 A
79	1.00 MeV	2.308E−01	1.681E−04	20.25 um	8773 A	7449 A
80	1.10 MeV	2.200E−01	1.547E−04	23.49 um	1.00 um	8469 A
81	1.20 MeV	2.094E−01	1.434E−04	26.88 um	1.13 um	9530 A
82	1.30 MeV	1.990E−01	1.337E−04	30.44 um	1.25 um	1.06 um
83	1.40 MeV	1.897E−01	1.253E−04	34.19 um	1.38 um	1.18 um
84	1.50 MeV	1.813E−01	1.180E−04	38.12 um	1.50 um	1.30 um
85	1.60 MeV	1.736E−01	1.115E−04	42.22 um	1.63 um	1.42 um

86	1.70 MeV	1.666E−01	1.057E−04	46.50 um	1.76 um	1.55 um
87	1.80 MeV	1.601E−01	1.005E−04	50.96 um	1.89 um	1.68 um
88	2.00 MeV	1.486E−01	9.161E−05	60.40 um	2.35 um	1.96 um
89	2.25 MeV	1.363E−01	8.257E−05	73.20 um	3.01 um	2.34 um
90	2.50 MeV	1.261E−01	7.523E−05	87.09 um	3.64 um	2.74 um
91	2.75 MeV	1.174E−01	6.914E−05	102.05 um	4.26 um	3.17 um
92	3.00 MeV	1.099E−01	6.401E−05	118.08 um	4.88 um	3.63 um
93	3.25 MeV	1.034E−01	5.962E−05	135.17 um	5.50 um	4.11 um
94	3.50 MeV	9.772E−02	5.582E−05	153.28 um	6.13 um	4.62 um
95	3.75 MeV	9.267E−02	5.250E−05	172.42 um	6.76 um	5.16 um
96	4.00 MeV	8.816E−02	4.957E−05	192.57 um	7.40 um	5.73 um
97	4.50 MeV	8.046E−02	4.463E−05	235.82 um	9.72 um	6.93 um
98	5.00 MeV	7.410E−02	4.063E−05	283.00 um	11.92 um	8.24 um
99	5.50 MeV	6.876E−02	3.731E−05	334.04 um	14.07 um	9.64 um
100	6.00 MeV	6.420E−02	3.451E−05	388.88 um	16.21 um	11.14 um
101	6.50 MeV	6.025E−02	3.213E−05	447.46 um	18.36 um	12.74 um
102	7.00 MeV	5.681E−02	3.006E−05	509.73 um	20.53 um	14.42 um
103	8.00 MeV	5.106E−02	2.667E−05	645.05 um	28.37 um	18.08 um
104	9.00 MeV	4.646E−02	2.399E−05	794.67 um	35.72 um	22.09 um
105	10.00 MeV	4.269E−02	2.182E−05	958.31 um	42.91 um	26.46 um
106	11.00 MeV	3.953E−02	2.002E−05	1.14 mm	50.09 um	31.17 um
107	12.00 MeV	3.684E−02	1.851E−05	1.33 mm	57.33 um	36.22 um
108	13.00 MeV	3.453E−02	1.722E−05	1.53 mm	64.65 um	41.60 um
109	14.00 MeV	3.251E−02	1.610E−05	1.75 mm	72.08 um	47.31 um
110	15.00 MeV	3.074E−02	1.513E−05	1.98 mm	79.64 um	53.34 um
111	16.00 MeV	2.917E−02	1.427E−05	2.22 mm	87.33 um	59.69 um
112	17.00 MeV	2.776E−02	1.351E−05	2.48 mm	95.15 um	66.35 um
113	18.00 MeV	2.650E−02	1.283E−05	2.75 mm	103.10 um	73.31 um
114	20.00 MeV	2.432E−02	1.166E−05	3.32 mm	132.44 um	88.16 um
115	22.50 MeV	2.210E−02	1.048E−05	4.11 mm	174.40 um	108.40 um
116	25.00 MeV	2.028E−02	9.520E−06	4.97 mm	214.28 um	130.44 um
117	27.50 MeV	1.877E−02	8.730E−06	5.90 mm	253.43 um	154.25 um
118	30.00 MeV	1.749E−02	8.065E−06	6.91 mm	292.48 um	179.78 um
119	32.50 MeV	1.639E−02	7.498E−06	7.98 mm	331.72 um	206.99 um
120	35.00 MeV	1.544E−02	7.008E−06	9.13 mm	371.34 um	235.84 um
121	37.50 MeV	1.460E−02	6.581E−06	10.34 mm	411.43 um	266.31 um
122	40.00 MeV	1.386E−02	6.204E−06	11.62 mm	452.05 um	298.36 um
123	45.00 MeV	1.261E−02	5.572E−06	14.38 mm	601.58 um	367.09 um
124	50.00 MeV	1.160E−02	5.060E−06	17.40 mm	742.19 um	441.81 um
125	55.00 MeV	1.075E−02	4.637E−06	20.66 mm	879.34 um	522.30 um
126	60.00 MeV	1.004E−02	4.282E−06	24.17 mm	1.02 mm	608.37 um
127	65.00 MeV	9.428E−03	3.980E−06	27.92 mm	1.15 mm	699.84 um
128	70.00 MeV	8.899E−03	3.718E−06	31.89 mm	1.29 mm	796.54 um
129	80.00 MeV	8.028E−03	3.289E−06	40.52 mm	1.79 mm	1.01 mm
130	90.00 MeV	7.340E−03	2.952E−06	50.02 mm	2.25 mm	1.23 mm
131	100.00 MeV	6.782E−03	2.680E−06	60.35 mm	2.69 mm	1.48 mm
132	110.00 MeV	6.320E−03	2.455E−06	71.49 mm	3.14 mm	1.74 mm
133	120.00 MeV	5.931E−03	2.266E−06	83.40 mm	3.58 mm	2.02 mm
134	130.00 MeV	5.599E−03	2.105E−06	96.05 mm	4.02 mm	2.31 mm
135	140.00 MeV	5.312E−03	1.966E−06	109.42 mm	4.46 mm	2.62 mm
136	150.00 MeV	5.062E−03	1.845E−06	123.48 mm	4.90 mm	2.95 mm
137	160.00 MeV	4.841E−03	1.738E−06	138.21 mm	5.35 mm	3.28 mm
138	170.00 MeV	4.646E−03	1.644E−06	153.58 mm	5.79 mm	3.63 mm
139	180.00 MeV	4.471E−03	1.559E−06	169.58 mm	6.24 mm	3.99 mm
140	200.00 MeV	4.173E−03	1.415E−06	203.34 mm	7.90 mm	4.75 mm
141	225.00 MeV	3.872E−03	1.269E−06	248.70 mm	10.23 mm	5.75 mm
142	250.00 MeV	3.630E−03	1.151E−06	297.33 mm	12.38 mm	6.81 mm

```
275.00 MeV   3.431E-03  1.054E-06  349.00 mm    14.43 mm     7.92 mm
300.00 MeV   3.264E-03  9.724E-07  403.48 mm    16.42 mm     9.07 mm
325.00 MeV   3.124E-03  9.029E-07  460.57 mm    18.36 mm    10.27 mm
350.00 MeV   3.003E-03  8.430E-07  520.10 mm    20.26 mm    11.50 mm
375.00 MeV   2.898E-03  7.907E-07  581.89 mm    22.13 mm    12.76 mm
400.00 MeV   2.807E-03  7.448E-07  645.81 mm    23.98 mm    14.05 mm
450.00 MeV   2.656E-03  6.677E-07  779.38 mm    30.65 mm    16.70 mm
500.00 MeV   2.535E-03  6.055E-07  919.93 mm    36.65 mm    19.43 mm
550.00 MeV   2.438E-03  5.542E-07    1.07 m     42.24 mm    22.21 mm
600.00 MeV   2.358E-03  5.111E-07    1.22 m     47.53 mm    25.04 mm
650.00 MeV   2.291E-03  4.745E-07    1.38 m     52.58 mm    27.90 mm
700.00 MeV   2.235E-03  4.428E-07    1.54 m     57.44 mm    30.78 mm
800.00 MeV   2.146E-03  3.911E-07    1.87 m     74.51 mm    36.58 mm
900.00 MeV   2.079E-03  3.505E-07    2.22 m     89.31 mm    42.37 mm
  1.00 GeV   2.028E-03  3.177E-07    2.57 m    102.68 mm    48.14 mm

Multiply Stopping by       for Stopping Units
-------------------       ------------------
 1.3700E+01                eV / Angstrom
 1.3700E+02               keV / micron
 1.3700E+02               MeV / mm
 1.0000E+00               keV / (ug/cm2)
 1.0000E+00               MeV / (mg/cm2)
 1.0000E+03               keV / (mg/cm2)
 1.5437E+01                eV / (1E15 atoms/cm2)
 7.6339E+00               L.S.S. reduced units
==============================================================
(C) 1984,1989,1992,1998,2008 by J.P. Biersack and J.F. Ziegler
```

Listing 3: Ion stopping and range tables of protons in carbon composite.

```
==========================================================================
               SRIM version ---> SRIM-2013.00
               Calc. date   ---> July 29, 2020
==========================================================================

Disk File Name = SRIM Outputs\Hydrogen in Carbon Composite.txt

Ion = Hydrogen [1] , Mass = 1.008 amu

Target Density =  1.5000E+00 g/cm3 = 9.3466E+22 atoms/cm3
======= Target  Composition ========
   Atom    Atom    Atomic     Mass
   Name    Numb    Percent    Percent
   ----    ----    -------    -------
     H       1     022.62     002.36
     C       6     073.81     091.73
     O       8     003.57     005.91
====================================
Bragg Correction = -3.61%
Stopping Units =  MeV / (mg/cm2)
See bottom of Table for other Stopping units

      Ion          dE/dx        dE/dx      Projected   Longitudinal    Lateral
     Energy        Elec.        Nuclear      Range      Straggling    Straggling
 ------------  ------------  ------------  ----------  -----------  -----------
 10.00 keV    4.274E-01  6.617E-03    1799 A       467 A        488 A
```

11.00	keV	4.458E−01	6.196E−03	1936	A	480 A	507 A
12.00	keV	4.629E−01	5.832E−03	2068	A	492 A	526 A
13.00	keV	4.790E−01	5.512E−03	2197	A	502 A	542 A
14.00	keV	4.942E−01	5.230E−03	2323	A	512 A	558 A
15.00	keV	5.085E−01	4.978E−03	2446	A	521 A	573 A
16.00	keV	5.219E−01	4.752E−03	2566	A	529 A	587 A
17.00	keV	5.347E−01	4.548E−03	2684	A	536 A	600 A
18.00	keV	5.467E−01	4.363E−03	2799	A	543 A	612 A
20.00	keV	5.689E−01	4.038E−03	3024	A	557 A	636 A
22.50	keV	5.936E−01	3.701E−03	3295	A	571 A	662 A
25.00	keV	6.154E−01	3.421E−03	3558	A	584 A	686 A
27.50	keV	6.346E−01	3.184E−03	3813	A	596 A	707 A
30.00	keV	6.517E−01	2.981E−03	4063	A	607 A	727 A
32.50	keV	6.670E−01	2.804E−03	4306	A	616 A	746 A
35.00	keV	6.806E−01	2.649E−03	4545	A	625 A	764 A
37.50	keV	6.929E−01	2.512E−03	4781	A	634 A	780 A
40.00	keV	7.038E−01	2.390E−03	5013	A	641 A	796 A
45.00	keV	7.224E−01	2.180E−03	5468	A	657 A	825 A
50.00	keV	7.372E−01	2.007E−03	5914	A	671 A	852 A
55.00	keV	7.487E−01	1.862E−03	6353	A	684 A	877 A
60.00	keV	7.573E−01	1.738E−03	6787	A	696 A	901 A
65.00	keV	7.633E−01	1.631E−03	7218	A	708 A	923 A
70.00	keV	7.669E−01	1.537E−03	7647	A	719 A	944 A
80.00	keV	7.684E−01	1.381E−03	8502	A	744 A	985 A
90.00	keV	7.635E−01	1.256E−03	9362	A	767 A	1023 A
100.00	keV	7.541E−01	1.153E−03	1.02	um	790 A	1059 A
110.00	keV	7.414E−01	1.067E−03	1.11	um	812 A	1095 A
120.00	keV	7.267E−01	9.934E−04	1.20	um	834 A	1130 A
130.00	keV	7.107E−01	9.302E−04	1.29	um	856 A	1165 A
140.00	keV	6.941E−01	8.751E−04	1.39	um	878 A	1200 A
150.00	keV	6.774E−01	8.267E−04	1.48	um	900 A	1234 A
160.00	keV	6.607E−01	7.837E−04	1.58	um	922 A	1270 A
170.00	keV	6.444E−01	7.452E−04	1.68	um	945 A	1305 A
180.00	keV	6.285E−01	7.107E−04	1.79	um	968 A	1341 A
200.00	keV	5.985E−01	6.509E−04	2.00	um	1038 A	1414 A
225.00	keV	5.644E−01	5.898E−04	2.29	um	1141 A	1510 A
250.00	keV	5.339E−01	5.399E−04	2.59	um	1247 A	1610 A
275.00	keV	5.068E−01	4.983E−04	2.91	um	1354 A	1714 A
300.00	keV	4.826E−01	4.630E−04	3.25	um	1464 A	1824 A
325.00	keV	4.609E−01	4.326E−04	3.60	um	1576 A	1939 A
350.00	keV	4.414E−01	4.063E−04	3.97	um	1691 A	2058 A
375.00	keV	4.238E−01	3.831E−04	4.35	um	1807 A	2183 A
400.00	keV	4.078E−01	3.626E−04	4.75	um	1925 A	2312 A
450.00	keV	3.798E−01	3.280E−04	5.59	um	2325 A	2586 A
500.00	keV	3.561E−01	2.997E−04	6.50	um	2714 A	2878 A
550.00	keV	3.358E−01	2.761E−04	7.46	um	3096 A	3188 A
600.00	keV	3.182E−01	2.562E−04	8.47	um	3477 A	3515 A
650.00	keV	3.027E−01	2.392E−04	9.54	um	3858 A	3859 A
700.00	keV	2.891E−01	2.243E−04	10.67	um	4240 A	4218 A
800.00	keV	2.660E−01	1.999E−04	13.06	um	5550 A	4980 A
900.00	keV	2.473E−01	1.805E−04	15.66	um	6774 A	5798 A
1.00	MeV	2.319E−01	1.647E−04	18.43	um	7956 A	6666 A
1.10	MeV	2.203E−01	1.515E−04	21.37	um	9109 A	7578 A
1.20	MeV	2.089E−01	1.405E−04	24.47	um	1.02 um	8530 A
1.30	MeV	1.982E−01	1.310E−04	27.74	um	1.14 um	9524 A
1.40	MeV	1.888E−01	1.227E−04	31.18	um	1.25 um	1.06 um
1.50	MeV	1.803E−01	1.155E−04	34.78	um	1.37 um	1.16 um

84	1.60 MeV	1.725E−01	1.092E−04	38.55 um	1.48 um	1.28 um
85	1.70 MeV	1.655E−01	1.035E−04	42.49 um	1.60 um	1.39 um
86	1.80 MeV	1.590E−01	9.845E−05	46.59 um	1.72 um	1.51 um
87	2.00 MeV	1.474E−01	8.973E−05	55.28 um	2.15 um	1.77 um
88	2.25 MeV	1.353E−01	8.087E−05	67.06 um	2.76 um	2.11 um
89	2.50 MeV	1.251E−01	7.368E−05	79.84 um	3.34 um	2.47 um
90	2.75 MeV	1.165E−01	6.772E−05	93.61 um	3.91 um	2.86 um
91	3.00 MeV	1.091E−01	6.270E−05	108.37 um	4.48 um	3.28 um
92	3.25 MeV	1.027E−01	5.840E−05	124.08 um	5.05 um	3.72 um
93	3.50 MeV	9.702E−02	5.468E−05	140.75 um	5.63 um	4.18 um
94	3.75 MeV	9.202E−02	5.142E−05	158.35 um	6.21 um	4.67 um
95	4.00 MeV	8.755E−02	4.855E−05	176.89 um	6.80 um	5.18 um
96	4.50 MeV	7.990E−02	4.371E−05	216.67 um	8.93 um	6.28 um
97	5.00 MeV	7.359E−02	3.979E−05	260.07 um	10.95 um	7.46 um
98	5.50 MeV	6.829E−02	3.654E−05	307.01 um	12.93 um	8.74 um
99	6.00 MeV	6.376E−02	3.381E−05	357.44 um	14.90 um	10.10 um
100	6.50 MeV	5.985E−02	3.147E−05	411.31 um	16.87 um	11.55 um
101	7.00 MeV	5.642E−02	2.944E−05	468.57 um	18.87 um	13.08 um
102	8.00 MeV	5.072E−02	2.612E−05	593.00 um	26.07 um	16.40 um
103	9.00 MeV	4.615E−02	2.349E−05	730.58 um	32.82 um	20.04 um
104	10.00 MeV	4.240E−02	2.137E−05	881.06 um	39.44 um	24.00 um
105	11.00 MeV	3.926E−02	1.961E−05	1.04 mm	46.03 um	28.28 um
106	12.00 MeV	3.659E−02	1.813E−05	1.22 mm	52.68 um	32.86 um
107	13.00 MeV	3.430E−02	1.687E−05	1.41 mm	59.41 um	37.74 um
108	14.00 MeV	3.229E−02	1.577E−05	1.61 mm	66.24 um	42.92 um
109	15.00 MeV	3.053E−02	1.482E−05	1.82 mm	73.18 um	48.39 um
110	16.00 MeV	2.897E−02	1.398E−05	2.04 mm	80.24 um	54.15 um
111	17.00 MeV	2.758E−02	1.323E−05	2.28 mm	87.42 um	60.19 um
112	18.00 MeV	2.632E−02	1.256E−05	2.53 mm	94.73 um	66.51 um
113	20.00 MeV	2.416E−02	1.142E−05	3.05 mm	121.70 um	79.98 um
114	22.50 MeV	2.195E−02	1.026E−05	3.78 mm	160.28 um	98.34 um
115	25.00 MeV	2.015E−02	9.324E−06	4.57 mm	196.93 um	118.33 um
116	27.50 MeV	1.864E−02	8.550E−06	5.43 mm	232.91 um	139.93 um
117	30.00 MeV	1.737E−02	7.899E−06	6.35 mm	268.80 um	163.09 um
118	32.50 MeV	1.628E−02	7.344E−06	7.34 mm	304.86 um	187.77 um
119	35.00 MeV	1.533E−02	6.864E−06	8.40 mm	341.27 um	213.95 um
120	37.50 MeV	1.450E−02	6.445E−06	9.51 mm	378.11 um	241.59 um
121	40.00 MeV	1.377E−02	6.077E−06	10.69 mm	415.43 um	270.66 um
122	45.00 MeV	1.253E−02	5.457E−06	13.22 mm	552.91 um	333.01 um
123	50.00 MeV	1.152E−02	4.956E−06	16.00 mm	682.17 um	400.79 um
124	55.00 MeV	1.068E−02	4.542E−06	19.00 mm	808.24 um	473.81 um
125	60.00 MeV	9.970E−03	4.194E−06	22.22 mm	933.28 um	551.88 um
126	65.00 MeV	9.364E−03	3.898E−06	25.67 mm	1.06 mm	634.86 um
127	70.00 MeV	8.839E−03	3.642E−06	29.33 mm	1.18 mm	722.58 um
128	80.00 MeV	7.973E−03	3.222E−06	37.26 mm	1.64 mm	911.73 um
129	90.00 MeV	7.290E−03	2.892E−06	46.00 mm	2.07 mm	1.12 mm
130	100.00 MeV	6.735E−03	2.625E−06	55.50 mm	2.48 mm	1.34 mm
131	110.00 MeV	6.276E−03	2.404E−06	65.74 mm	2.88 mm	1.58 mm
132	120.00 MeV	5.890E−03	2.219E−06	76.70 mm	3.29 mm	1.83 mm
133	130.00 MeV	5.560E−03	2.062E−06	88.33 mm	3.69 mm	2.10 mm
134	140.00 MeV	5.275E−03	1.926E−06	100.63 mm	4.10 mm	2.38 mm
135	150.00 MeV	5.026E−03	1.807E−06	113.56 mm	4.51 mm	2.67 mm
136	160.00 MeV	4.807E−03	1.703E−06	127.11 mm	4.91 mm	2.98 mm
137	170.00 MeV	4.613E−03	1.610E−06	141.25 mm	5.33 mm	3.29 mm
138	180.00 MeV	4.439E−03	1.527E−06	155.97 mm	5.74 mm	3.62 mm
139	200.00 MeV	4.143E−03	1.386E−06	187.03 mm	7.27 mm	4.31 mm
140	225.00 MeV	3.844E−03	1.243E−06	228.76 mm	9.41 mm	5.22 mm

```
250.00 MeV   3.603E-03  1.127E-06  273.51 mm    11.39 mm     6.18 mm
275.00 MeV   3.405E-03  1.032E-06  321.05 mm    13.27 mm     7.18 mm
300.00 MeV   3.240E-03  9.523E-07  371.19 mm    15.10 mm     8.23 mm
325.00 MeV   3.100E-03  8.843E-07  423.73 mm    16.89 mm     9.32 mm
350.00 MeV   2.980E-03  8.256E-07  478.52 mm    18.64 mm    10.43 mm
375.00 MeV   2.876E-03  7.744E-07  535.41 mm    20.36 mm    11.58 mm
400.00 MeV   2.785E-03  7.295E-07  594.25 mm    22.06 mm    12.75 mm
450.00 MeV   2.634E-03  6.539E-07  717.24 mm    28.20 mm    15.16 mm
500.00 MeV   2.514E-03  5.930E-07  846.67 mm    33.73 mm    17.64 mm
550.00 MeV   2.417E-03  5.428E-07  981.79 mm    38.88 mm    20.17 mm
600.00 MeV   2.337E-03  5.006E-07    1.12 m     43.76 mm    22.74 mm
650.00 MeV   2.271E-03  4.647E-07    1.27 m     48.41 mm    25.34 mm
700.00 MeV   2.214E-03  4.337E-07    1.42 m     52.89 mm    27.97 mm
800.00 MeV   2.125E-03  3.830E-07    1.72 m     68.64 mm    33.24 mm
900.00 MeV   2.059E-03  3.432E-07    2.04 m     82.30 mm    38.52 mm
  1.00 GeV   2.008E-03  3.111E-07    2.37 m     94.64 mm    43.77 mm

 Multiply Stopping by        for Stopping Units
 -------------------        ------------------
  1.5000E+01                 eV / Angstrom
  1.5000E+02                keV / micron
  1.5000E+02                MeV / mm
  1.0000E+00                keV / (ug/cm2)
  1.0000E+00                MeV / (mg/cm2)
  1.0000E+03                keV / (mg/cm2)
  1.6048E+01                 eV / (1E15 atoms/cm2)
  8.0274E+00                L.S.S. reduced units
 ================================================================
 (C) 1984,1989,1992,1998,2008 by J.P. Biersack and J.F. Ziegler
```

Listing 4: Ion stopping and range tables of protons in aluminum.

```
 ==========================================================
              SRIM version ---> SRIM-2013.00
              Calc. date   ---> July 29, 2020
 ==========================================================

 Disk File Name = SRIM Outputs\Hydrogen in Aluminum.txt

 Ion = Hydrogen [1] , Mass = 1.008 amu

 Target Density =  2.7020E+00 g/cm3 = 6.0305E+22 atoms/cm3
 ======= Target  Composition ========
    Atom    Atom    Atomic     Mass
    Name    Numb    Percent    Percent
    ----    ----    -------    -------
     Al      13     100.00     100.00
 ====================================
 Bragg Correction = 0.00%
 Stopping Units =  MeV / (mg/cm2)
 See bottom of Table for other Stopping units

       Ion          dE/dx       dE/dx      Projected   Longitudinal    Lateral
      Energy        Elec.       Nuclear      Range      Straggling    Straggling
 ---------------  ----------  ----------  ----------  ------------  ------------
  10.00 keV    2.797E-01  4.085E-03    1277 A        501 A         471 A
  11.00 keV    2.924E-01  3.861E-03    1382 A        518 A         493 A
```

12.00	keV	3.044E−01	3.664E−03	1484	A	534 A	514 A
13.00	keV	3.155E−01	3.489E−03	1583	A	549 A	534 A
14.00	keV	3.260E−01	3.332E−03	1681	A	563 A	552 A
15.00	keV	3.359E−01	3.190E−03	1776	A	575 A	570 A
16.00	keV	3.451E−01	3.062E−03	1869	A	587 A	586 A
17.00	keV	3.537E−01	2.945E−03	1961	A	598 A	602 A
18.00	keV	3.618E−01	2.838E−03	2052	A	608 A	617 A
20.00	keV	3.766E−01	2.648E−03	2229	A	628 A	645 A
22.50	keV	3.925E−01	2.448E−03	2444	A	649 A	678 A
25.00	keV	4.062E−01	2.279E−03	2653	A	668 A	708 A
27.50	keV	4.178E−01	2.135E−03	2858	A	685 A	735 A
30.00	keV	4.276E−01	2.010E−03	3059	A	701 A	761 A
32.50	keV	4.360E−01	1.900E−03	3257	A	716 A	786 A
35.00	keV	4.430E−01	1.803E−03	3453	A	729 A	809 A
37.50	keV	4.489E−01	1.717E−03	3647	A	742 A	831 A
40.00	keV	4.538E−01	1.639E−03	3839	A	754 A	852 A
45.00	keV	4.612E−01	1.505E−03	4220	A	777 A	893 A
50.00	keV	4.658E−01	1.394E−03	4599	A	798 A	931 A
55.00	keV	4.685E−01	1.299E−03	4977	A	818 A	967 A
60.00	keV	4.695E−01	1.218E−03	5354	A	837 A	1002 A
65.00	keV	4.692E−01	1.147E−03	5733	A	855 A	1035 A
70.00	keV	4.680E−01	1.085E−03	6113	A	872 A	1068 A
80.00	keV	4.636E−01	9.803E−04	6880	A	907 A	1131 A
90.00	keV	4.573E−01	8.958E−04	7660	A	941 A	1192 A
100.00	keV	4.499E−01	8.259E−04	8453	A	973 A	1252 A
110.00	keV	4.420E−01	7.670E−04	9262	A	1005 A	1311 A
120.00	keV	4.338E−01	7.166E−04	1.01	um	1036 A	1370 A
130.00	keV	4.256E−01	6.730E−04	1.09	um	1067 A	1429 A
140.00	keV	4.175E−01	6.348E−04	1.18	um	1098 A	1487 A
150.00	keV	4.095E−01	6.011E−04	1.27	um	1128 A	1546 A
160.00	keV	4.017E−01	5.711E−04	1.36	um	1159 A	1604 A
170.00	keV	3.941E−01	5.442E−04	1.45	um	1189 A	1664 A
180.00	keV	3.868E−01	5.199E−04	1.54	um	1220 A	1723 A
200.00	keV	3.730E−01	4.777E−04	1.73	um	1295 A	1844 A
225.00	keV	3.571E−01	4.345E−04	1.98	um	1399 A	1998 A
250.00	keV	3.427E−01	3.989E−04	2.24	um	1503 A	2155 A
275.00	keV	3.297E−01	3.691E−04	2.51	um	1608 A	2317 A
300.00	keV	3.178E−01	3.438E−04	2.80	um	1714 A	2483 A
325.00	keV	3.069E−01	3.219E−04	3.09	um	1822 A	2652 A
350.00	keV	2.969E−01	3.029E−04	3.39	um	1930 A	2826 A
375.00	keV	2.877E−01	2.862E−04	3.71	um	2040 A	3004 A
400.00	keV	2.792E−01	2.713E−04	4.03	um	2151 A	3186 A
450.00	keV	2.640E−01	2.460E−04	4.70	um	2469 A	3561 A
500.00	keV	2.508E−01	2.254E−04	5.42	um	2783 A	3952 A
550.00	keV	2.392E−01	2.081E−04	6.16	um	3095 A	4358 A
600.00	keV	2.289E−01	1.935E−04	6.95	um	3407 A	4777 A
650.00	keV	2.197E−01	1.809E−04	7.77	um	3719 A	5211 A
700.00	keV	2.115E−01	1.700E−04	8.62	um	4033 A	5657 A
800.00	keV	1.972E−01	1.518E−04	10.42	um	4996 A	6588 A
900.00	keV	1.852E−01	1.374E−04	12.34	um	5916 A	7566 A
1.00	MeV	1.749E−01	1.256E−04	14.38	um	6815 A	8590 A
1.10	MeV	1.654E−01	1.158E−04	16.54	um	7707 A	9659 A
1.20	MeV	1.558E−01	1.075E−04	18.83	um	8608 A	1.08 um
1.30	MeV	1.478E−01	1.004E−04	21.26	um	9522 A	1.20 um
1.40	MeV	1.408E−01	9.421E−05	23.81	um	1.04 um	1.32 um
1.50	MeV	1.346E−01	8.879E−05	26.48	um	1.14 um	1.44 um
1.60	MeV	1.289E−01	8.399E−05	29.27	um	1.23 um	1.58 um

83	1.70 MeV	1.238E−01	7.971E−05	32.19 um	1.33 um	1.71 um
84	1.80 MeV	1.191E−01	7.587E−05	35.22 um	1.43 um	1.86 um
85	2.00 MeV	1.108E−01	6.927E−05	41.63 um	1.75 um	2.15 um
86	2.25 MeV	1.021E−01	6.254E−05	50.28 um	2.21 um	2.55 um
87	2.50 MeV	9.486E−02	5.707E−05	59.64 um	2.65 um	2.98 um
88	2.75 MeV	8.868E−02	5.253E−05	69.67 um	3.08 um	3.43 um
89	3.00 MeV	8.336E−02	4.869E−05	80.38 um	3.51 um	3.91 um
90	3.25 MeV	7.871E−02	4.540E−05	91.75 um	3.95 um	4.41 um
91	3.50 MeV	7.461E−02	4.255E−05	103.77 um	4.39 um	4.95 um
92	3.75 MeV	7.097E−02	4.006E−05	116.42 um	4.83 um	5.50 um
93	4.00 MeV	6.771E−02	3.785E−05	129.71 um	5.29 um	6.08 um
94	4.50 MeV	6.210E−02	3.413E−05	158.13 um	6.82 um	7.32 um
95	5.00 MeV	5.744E−02	3.111E−05	188.98 um	8.29 um	8.65 um
96	5.50 MeV	5.350E−02	2.860E−05	222.22 um	9.73 um	10.07 um
97	6.00 MeV	5.013E−02	2.649E−05	257.80 um	11.17 um	11.58 um
98	6.50 MeV	4.719E−02	2.468E−05	295.69 um	12.62 um	13.19 um
99	7.00 MeV	4.462E−02	2.311E−05	335.85 um	14.08 um	14.88 um
100	8.00 MeV	4.031E−02	2.053E−05	422.78 um	19.13 um	18.51 um
101	9.00 MeV	3.683E−02	1.849E−05	518.46 um	23.90 um	22.48 um
102	10.00 MeV	3.396E−02	1.684E−05	622.71 um	28.58 um	26.77 um
103	11.00 MeV	3.155E−02	1.547E−05	735.35 um	33.27 um	31.38 um
104	12.00 MeV	2.949E−02	1.431E−05	856.24 um	37.99 um	36.29 um
105	13.00 MeV	2.771E−02	1.333E−05	985.24 um	42.77 um	41.51 um
106	14.00 MeV	2.615E−02	1.247E−05	1.12 mm	47.64 um	47.03 um
107	15.00 MeV	2.478E−02	1.173E−05	1.27 mm	52.58 um	52.84 um
108	16.00 MeV	2.355E−02	1.107E−05	1.42 mm	57.62 um	58.94 um
109	17.00 MeV	2.246E−02	1.048E−05	1.58 mm	62.74 um	65.33 um
110	18.00 MeV	2.147E−02	9.958E−06	1.75 mm	67.96 um	71.99 um
111	20.00 MeV	1.976E−02	9.060E−06	2.11 mm	86.39 um	86.15 um
112	22.50 MeV	1.801E−02	8.150E−06	2.59 mm	112.65 um	105.35 um
113	25.00 MeV	1.658E−02	7.412E−06	3.13 mm	137.73 um	126.20 um
114	27.50 MeV	1.538E−02	6.803E−06	3.71 mm	162.44 um	148.63 um
115	30.00 MeV	1.436E−02	6.289E−06	4.33 mm	187.12 um	172.61 um
116	32.50 MeV	1.348E−02	5.851E−06	4.99 mm	211.97 um	198.10 um
117	35.00 MeV	1.271E−02	5.472E−06	5.69 mm	237.08 um	225.06 um
118	37.50 MeV	1.204E−02	5.141E−06	6.44 mm	262.53 um	253.48 um
119	40.00 MeV	1.145E−02	4.850E−06	7.23 mm	288.35 um	283.31 um
120	45.00 MeV	1.044E−02	4.359E−06	8.91 mm	380.32 um	347.11 um
121	50.00 MeV	9.619E−03	3.962E−06	10.75 mm	467.27 um	416.26 um
122	55.00 MeV	8.934E−03	3.634E−06	12.74 mm	552.34 um	490.56 um
123	60.00 MeV	8.354E−03	3.358E−06	14.88 mm	636.88 um	569.82 um
124	65.00 MeV	7.857E−03	3.122E−06	17.16 mm	721.60 um	653.89 um
125	70.00 MeV	7.425E−03	2.919E−06	19.57 mm	806.87 um	742.61 um
126	80.00 MeV	6.713E−03	2.585E−06	24.80 mm	1.11 mm	933.43 um
127	90.00 MeV	6.148E−03	2.321E−06	30.55 mm	1.39 mm	1.14 mm
128	100.00 MeV	5.689E−03	2.109E−06	36.79 mm	1.67 mm	1.37 mm
129	110.00 MeV	5.309E−03	1.933E−06	43.50 mm	1.94 mm	1.60 mm
130	120.00 MeV	4.988E−03	1.785E−06	50.68 mm	2.21 mm	1.86 mm
131	130.00 MeV	4.714E−03	1.659E−06	58.29 mm	2.48 mm	2.12 mm
132	140.00 MeV	4.477E−03	1.550E−06	66.33 mm	2.75 mm	2.40 mm
133	150.00 MeV	4.269E−03	1.456E−06	74.77 mm	3.02 mm	2.70 mm
134	160.00 MeV	4.087E−03	1.372E−06	83.61 mm	3.30 mm	3.00 mm
135	170.00 MeV	3.925E−03	1.298E−06	92.82 mm	3.57 mm	3.31 mm
136	180.00 MeV	3.780E−03	1.232E−06	102.41 mm	3.85 mm	3.64 mm
137	200.00 MeV	3.532E−03	1.118E−06	122.62 mm	4.85 mm	4.32 mm
138	225.00 MeV	3.282E−03	1.004E−06	149.74 mm	6.25 mm	5.22 mm
139	250.00 MeV	3.080E−03	9.110E−07	178.77 mm	7.54 mm	6.16 mm

```
275.00 MeV   2.915E-03  8.345E-07  209.58 mm     8.78 mm     7.16 mm
300.00 MeV   2.776E-03  7.703E-07  242.04 mm     9.98 mm     8.19 mm
325.00 MeV   2.659E-03  7.156E-07  276.02 mm    11.16 mm     9.25 mm
350.00 MeV   2.558E-03  6.684E-07  311.42 mm    12.31 mm    10.35 mm
375.00 MeV   2.471E-03  6.272E-07  348.14 mm    13.44 mm    11.47 mm
400.00 MeV   2.395E-03  5.910E-07  386.09 mm    14.56 mm    12.62 mm
450.00 MeV   2.269E-03  5.301E-07  465.32 mm    18.53 mm    14.97 mm
500.00 MeV   2.169E-03  4.810E-07  548.58 mm    22.11 mm    17.39 mm
550.00 MeV   2.088E-03  4.404E-07  635.37 mm    25.44 mm    19.85 mm
600.00 MeV   2.022E-03  4.064E-07  725.26 mm    28.60 mm    22.35 mm
650.00 MeV   1.967E-03  3.774E-07  817.90 mm    31.62 mm    24.87 mm
700.00 MeV   1.920E-03  3.524E-07  912.96 mm    34.52 mm    27.41 mm
800.00 MeV   1.847E-03  3.114E-07    1.11 m     44.57 mm    32.50 mm
900.00 MeV   1.793E-03  2.792E-07    1.31 m     53.29 mm    37.58 mm
  1.00 GeV   1.752E-03  2.532E-07    1.52 m     61.17 mm    42.63 mm

 Multiply Stopping by        for Stopping Units
 ------------------------    ------------------------
  2.7019E+01                  eV / Angstrom
  2.7019E+02                 keV / micron
  2.7019E+02                 MeV / mm
  1.0000E+00                 keV / (ug/cm2)
  1.0000E+00                 MeV / (mg/cm2)
  1.0000E+03                 keV / (mg/cm2)
  4.4804E+01                  eV / (1E15 atoms/cm2)
  2.8899E+01                 L.S.S. reduced units
 ================================================================
 (C) 1984,1989,1992,1998,2008 by J.P. Biersack and J.F. Ziegler
```

B SPENVIS Output

Listing 5: ESP PSYCHIC SPE worst case 1 year.

```
'*',    54,    1,    25,    22,    5,    5,    75,    1
'SPENVIS 4.6.10.3408          - 23-Jul-2020 00:20:04'
'PRJ_DEF', -1,'TEST_PROJECT'
'PRJ_HDR', -1,'My Test Project'
'MOD_ABB', -1,'SEP'
'MIS_PLA',  1,   -3,' '
'MIS_NTR',  1,    1,' '
'MIS_STA',  1,  9862.00000000,' '
'MIS_END',  1, 15337.00000000,' '
'MIS_DUR',  1, 5.475000E+03,'days'
'SEP_IEL',  1,  1,' '
'SEP_JEL',  1,  1,' '
'SEP_MOD', -1,'ESP-PSYCHIC worst event fluence'
'SEP_TMI',  1,  1.0,'years'
'SEP_TMA',  1,  0.0,'years'
'SEP_DUR',  1,  1.0,'years'
'SEP_NCY',  1,  1,' '
'SEP_NOR',  1,  0,' '
'SEP_NAL',  1,  0,' '
'SEP_PRB',  1,  95.0,'%'
'SEP_OMN',  1, 1, ' '
```

```
'SEP_ABS',  -1,'Energy'
'SEP_IGC',   1,   0,' '
'SEP_IGV',   1,   1,' '
'SEP_IST',   1,   0,' '
'PLT_HDR',  -1,'ESP-PSYCHIC worst event fluence: solar protons'
'SPECIES',  -1,'proton'
'PS Annotation',   8,   1
'Mission start: 01/01/1977 00:00:00'
 0.05, 0.00, 0.00
'Mission end: 29/12/1991 00:00:00'
 0.95, 0.00, 1.00
'Nr. of segments:   1'
 0.05, 1.50, 0.00
'Duration: 5475.00 days'
 0.95, 0.00, 1.00
'PS Annotation',  12,   0
'Solar particle model: ESP-PSYCHIC worst event fluence'
 0.05, 2.00, 0.00
'Mission duration: 1.00 years, spanning 1 solar cycles'
 0.10, 1.50, 0.00
'1.00 years in solar maximum'
 0.15, 1.50, 0.00
'0.00 years in solar minimum'
 0.15, 1.50, 0.00
'Confidence level: 95.000%'
 0.10, 1.50, 0.00
'Magnetic shielding:    off'
 0.10, 1.50, 0.00
'Energy','MeV', 1,'Energy'
'IFlux','cm!u-2!n', 1,'Integral Fluence'
'DFlux','cm!u-2!n MeV!u-1!n', 1,'Differential Fluence'
'Attenuation',' ', 1,'Orbit Averaged Proton Attenuation Factor'
'Exposure','hrs', 1,'Proton Exposure Time'
  1.0000E-01,  4.9253E+11,  2.8327E+12, 1.0000, 1.3140E+05
  1.1000E-01,  4.6599E+11,  2.4764E+12, 1.0000, 1.3140E+05
  1.2000E-01,  4.4301E+11,  2.1650E+12, 1.0000, 1.3140E+05
  1.4000E-01,  4.0504E+11,  1.7055E+12, 1.0000, 1.3140E+05
  1.6000E-01,  3.7479E+11,  1.3763E+12, 1.0000, 1.3140E+05
  1.8000E-01,  3.4999E+11,  1.1398E+12, 1.0000, 1.3140E+05
  2.0000E-01,  3.2919E+11,  9.6334E+11, 1.0000, 1.3140E+05
  2.2000E-01,  3.1145E+11,  8.2966E+11, 1.0000, 1.3140E+05
  2.5000E-01,  2.8915E+11,  6.7898E+11, 1.0000, 1.3140E+05
  2.8000E-01,  2.7071E+11,  5.6775E+11, 1.0000, 1.3140E+05
  3.2000E-01,  2.5050E+11,  4.5880E+11, 1.0000, 1.3140E+05
  3.5000E-01,  2.3778E+11,  3.9807E+11, 1.0000, 1.3140E+05
  4.0000E-01,  2.2002E+11,  3.2318E+11, 1.0000, 1.3140E+05
  4.5000E-01,  2.0546E+11,  2.6766E+11, 1.0000, 1.3140E+05
  5.0000E-01,  1.9326E+11,  2.2622E+11, 1.0000, 1.3140E+05
  5.5000E-01,  1.8284E+11,  1.9492E+11, 1.0000, 1.3140E+05
  6.3000E-01,  1.6896E+11,  1.5763E+11, 1.0000, 1.3140E+05
  7.1000E-01,  1.5762E+11,  1.3030E+11, 1.0000, 1.3140E+05
  8.0000E-01,  1.4706E+11,  1.0787E+11, 1.0000, 1.3140E+05
  9.0000E-01,  1.3732E+11,  8.9447E+10, 1.0000, 1.3140E+05
  1.0000E+00,  1.2917E+11,  7.5598E+10, 1.0000, 1.3140E+05
  1.1000E+00,  1.2220E+11,  6.4944E+10, 1.0000, 1.3140E+05
  1.2000E+00,  1.1618E+11,  5.6777E+10, 1.0000, 1.3140E+05
  1.4000E+00,  1.0622E+11,  4.4726E+10, 1.0000, 1.3140E+05
```

```
  1.6000E+00,  9.8287E+10,  3.6093E+10, 1.0000, 1.3140E+05
  1.8000E+00,  9.1783E+10,  2.9892E+10, 1.0000, 1.3140E+05
  2.0000E+00,  8.6331E+10,  2.5264E+10, 1.0000, 1.3140E+05
  2.2000E+00,  8.1678E+10,  2.1758E+10, 1.0000, 1.3140E+05
  2.5000E+00,  7.5829E+10,  1.7806E+10, 1.0000, 1.3140E+05
  2.8000E+00,  7.0994E+10,  1.5325E+10, 1.0000, 1.3140E+05
  3.2000E+00,  6.5285E+10,  1.3442E+10, 1.0000, 1.3140E+05
  3.5000E+00,  6.1439E+10,  1.1998E+10, 1.0000, 1.3140E+05
  4.0000E+00,  5.6125E+10,  9.6194E+09, 1.0000, 1.3140E+05
  4.5000E+00,  5.1820E+10,  7.8751E+09, 1.0000, 1.3140E+05
  5.0000E+00,  4.8250E+10,  7.2806E+09, 1.0000, 1.3140E+05
  5.5000E+00,  4.4539E+10,  6.8738E+09, 1.0000, 1.3140E+05
  6.3000E+00,  3.9740E+10,  5.4586E+09, 1.0000, 1.3140E+05
  7.1000E+00,  3.5806E+10,  4.9353E+09, 1.0000, 1.3140E+05
  8.0000E+00,  3.1347E+10,  4.4340E+09, 1.0000, 1.3140E+05
  9.0000E+00,  2.7491E+10,  3.4506E+09, 1.0000, 1.3140E+05
  1.0000E+01,  2.4445E+10,  2.6797E+09, 1.0000, 1.3140E+05
  1.1000E+01,  2.2131E+10,  2.1174E+09, 1.0000, 1.3140E+05
  1.2000E+01,  2.0210E+10,  1.7809E+09, 1.0000, 1.3140E+05
  1.4000E+01,  1.7208E+10,  1.2866E+09, 1.0000, 1.3140E+05
  1.6000E+01,  1.5064E+10,  9.3293E+08, 1.0000, 1.3140E+05
  1.8000E+01,  1.3476E+10,  7.1663E+08, 1.0000, 1.3140E+05
  2.0000E+01,  1.2198E+10,  6.5060E+08, 1.0000, 1.3140E+05
  2.2000E+01,  1.0874E+10,  6.0432E+08, 1.0000, 1.3140E+05
  2.5000E+01,  9.3205E+09,  4.5508E+08, 1.0000, 1.3140E+05
  2.8000E+01,  8.1431E+09,  3.6265E+08, 1.0000, 1.3140E+05
  3.2000E+01,  6.8515E+09,  2.9247E+08, 1.0000, 1.3140E+05
  3.5000E+01,  6.0426E+09,  2.5867E+08, 1.0000, 1.3140E+05
  4.0000E+01,  4.8408E+09,  2.0982E+08, 1.0000, 1.3140E+05
  4.5000E+01,  3.9443E+09,  1.5897E+08, 1.0000, 1.3140E+05
  5.0000E+01,  3.2512E+09,  1.2647E+08, 1.0000, 1.3140E+05
  5.5000E+01,  2.6796E+09,  1.0417E+08, 1.0000, 1.3140E+05
  6.3000E+01,  1.9761E+09,  7.2882E+07, 1.0000, 1.3140E+05
  7.1000E+01,  1.5135E+09,  5.1021E+07, 1.0000, 1.3140E+05
  8.0000E+01,  1.1232E+09,  3.7228E+07, 1.0000, 1.3140E+05
  9.0000E+01,  8.1915E+08,  2.4763E+07, 1.0000, 1.3140E+05
  1.0000E+02,  6.2791E+08,  1.5663E+07, 1.0000, 1.3140E+05
  1.1000E+02,  5.0590E+08,  1.0628E+07, 1.0000, 1.3140E+05
  1.2000E+02,  4.1534E+08,  8.1466E+06, 1.0000, 1.3140E+05
  1.4000E+02,  2.8879E+08,  5.1594E+06, 1.0000, 1.3140E+05
  1.6000E+02,  2.0896E+08,  3.3143E+06, 1.0000, 1.3140E+05
  1.8000E+02,  1.5621E+08,  2.2258E+06, 1.0000, 1.3140E+05
  2.0000E+02,  1.1993E+08,  1.5600E+06, 1.0000, 1.3140E+05
  2.2000E+02,  9.3814E+07,  1.1385E+06, 1.0000, 1.3140E+05
  2.5000E+02,  6.7186E+07,  7.4414E+05, 1.0000, 1.3140E+05
  2.8000E+02,  4.9165E+07,  5.0590E+05, 1.0000, 1.3140E+05
  3.2000E+02,  3.3986E+07,  3.0472E+05, 1.0000, 1.3140E+05
  3.5000E+02,  2.6526E+07,  2.1683E+05, 1.0000, 1.3140E+05
  4.0000E+02,  1.8336E+07,  1.3287E+05, 1.0000, 1.3140E+05
  4.5000E+02,  1.3239E+07,  8.4433E+04, 1.0000, 1.3140E+05
  5.0000E+02,  9.8930E+06,  4.9413E+04, 1.0000, 1.3140E+05
'End of Block'
'*',    52,     1,     25,     22,     3,     3,     75,     0
'SPENVIS 4.6.10.3408 ---------- 23-Jul-2020 00:20:04'
'PRJ_DEF', -1,'TEST_PROJECT'
'PRJ_HDR', -1,'My Test Project'
'MOD_ABB', -1,'SEP'
```

```
'MIS_PLA',   1,    -3,'␣'
'MIS_NTR',   1,     1,'␣'
'MIS_STA',   1,    9862.00000000,'␣'
'MIS_END',   1,   15337.00000000,'␣'
'MIS_DUR',   1, 5.475000E+03,'days'
'SEP_IEL',   1,   1,'␣'
'SEP_JEL',   1,   1,'␣'
'SEP_MOD',  -1,'ESP-PSYCHIC␣worst␣event␣fluence'
'SEP_TMI',   1,   1.0,'years'
'SEP_TMA',   1,   0.0,'years'
'SEP_DUR',   1,   1.0,'years'
'SEP_NCY',   1,   1,'␣'
'SEP_NOR',   1,   0,'␣'
'SEP_NAL',   1,   0,'␣'
'SEP_PRB',   1,   95.0,'%'
'SEP_OMN',   1, 1,  '␣'
'SEP_ABS',  -1,'Energy'
'SEP_IGC',   1,   0,'␣'
'SEP_IGV',   1,   1,'␣'
'SEP_IST',   1,   0,'␣'
'PLT_HDR',  -1,'ESP-PSYCHIC␣worst␣event␣fluence:␣solar␣ions'
'SPECIES',  -1,'H␣'
'PS␣Annotation',   8,   1
'Mission␣start:␣01/01/1977␣00:00:00'
 0.05,  0.00,  0.00
'Mission␣end:␣29/12/1991␣00:00:00'
 0.95,  0.00,  1.00
'Nr.␣of␣segments:␣␣␣1'
 0.05,  1.50,  0.00
'Duration:␣5475.00␣days'
 0.95,  0.00,  1.00
'PS␣Annotation',  12,   0
'Solar␣particle␣model:␣ESP-PSYCHIC␣worst␣event␣fluence'
 0.05,  2.00,  0.00
'Mission␣duration:␣1.00␣years,␣spanning␣1␣solar␣cycles'
 0.10,  1.50,  0.00
'1.00␣years␣in␣solar␣maximum'
 0.15,  1.50,  0.00
'0.00␣years␣in␣solar␣minimum'
 0.15,  1.50,  0.00
'Confidence␣level:␣95.000%'
 0.10,  1.50,  0.00
'Magnetic␣shielding:␣␣␣␣off'
 0.10,  1.50,  0.00
'Energy','MeV/n',  1,'Energy'
'IFlux','cm!u-2!n',   1,'Integral␣Fluence␣of␣','SPECIES'
'DFlux','cm!u-2!n␣(MeV/n)!u-1!n',   1,'Differential␣Fluence␣of␣','SPECIES'
   1.0000E-01,   4.9253E+11,   2.8327E+12
   1.1000E-01,   4.6599E+11,   2.4764E+12
   1.2000E-01,   4.4301E+11,   2.1650E+12
   1.4000E-01,   4.0504E+11,   1.7055E+12
   1.6000E-01,   3.7479E+11,   1.3763E+12
   1.8000E-01,   3.4999E+11,   1.1398E+12
   2.0000E-01,   3.2919E+11,   9.6334E+11
   2.2000E-01,   3.1145E+11,   8.2966E+11
   2.5000E-01,   2.8915E+11,   6.7898E+11
   2.8000E-01,   2.7071E+11,   5.6775E+11
```

```
193   3.2000E-01,  2.5050E+11,  4.5880E+11
194   3.5000E-01,  2.3778E+11,  3.9807E+11
195   4.0000E-01,  2.2002E+11,  3.2318E+11
196   4.5000E-01,  2.0546E+11,  2.6766E+11
197   5.0000E-01,  1.9326E+11,  2.2622E+11
198   5.5000E-01,  1.8284E+11,  1.9492E+11
199   6.3000E-01,  1.6896E+11,  1.5763E+11
200   7.1000E-01,  1.5762E+11,  1.3030E+11
201   8.0000E-01,  1.4706E+11,  1.0787E+11
202   9.0000E-01,  1.3732E+11,  8.9447E+10
203   1.0000E+00,  1.2917E+11,  7.5598E+10
204   1.1000E+00,  1.2220E+11,  6.4944E+10
205   1.2000E+00,  1.1618E+11,  5.6777E+10
206   1.4000E+00,  1.0622E+11,  4.4726E+10
207   1.6000E+00,  9.8287E+10,  3.6093E+10
208   1.8000E+00,  9.1783E+10,  2.9892E+10
209   2.0000E+00,  8.6331E+10,  2.5264E+10
210   2.2000E+00,  8.1678E+10,  2.1758E+10
211   2.5000E+00,  7.5829E+10,  1.7806E+10
212   2.8000E+00,  7.0994E+10,  1.5325E+10
213   3.2000E+00,  6.5285E+10,  1.3442E+10
214   3.5000E+00,  6.1439E+10,  1.1998E+10
215   4.0000E+00,  5.6125E+10,  9.6194E+09
216   4.5000E+00,  5.1820E+10,  7.8751E+09
217   5.0000E+00,  4.8250E+10,  7.2806E+09
218   5.5000E+00,  4.4539E+10,  6.8738E+09
219   6.3000E+00,  3.9740E+10,  5.4586E+09
220   7.1000E+00,  3.5806E+10,  4.9353E+09
221   8.0000E+00,  3.1347E+10,  4.4340E+09
222   9.0000E+00,  2.7491E+10,  3.4506E+09
223   1.0000E+01,  2.4445E+10,  2.6797E+09
224   1.1000E+01,  2.2131E+10,  2.1174E+09
225   1.2000E+01,  2.0210E+10,  1.7809E+09
226   1.4000E+01,  1.7208E+10,  1.2866E+09
227   1.6000E+01,  1.5064E+10,  9.3293E+08
228   1.8000E+01,  1.3476E+10,  7.1663E+08
229   2.0000E+01,  1.2198E+10,  6.5060E+08
230   2.2000E+01,  1.0874E+10,  6.0432E+08
231   2.5000E+01,  9.3205E+09,  4.5508E+08
232   2.8000E+01,  8.1431E+09,  3.6265E+08
233   3.2000E+01,  6.8515E+09,  2.9247E+08
234   3.5000E+01,  6.0426E+09,  2.5867E+08
235   4.0000E+01,  4.8408E+09,  2.0982E+08
236   4.5000E+01,  3.9443E+09,  1.5897E+08
237   5.0000E+01,  3.2512E+09,  1.2647E+08
238   5.5000E+01,  2.6796E+09,  1.0417E+08
239   6.3000E+01,  1.9761E+09,  7.2882E+07
240   7.1000E+01,  1.5135E+09,  5.1021E+07
241   8.0000E+01,  1.1232E+09,  3.7228E+07
242   9.0000E+01,  8.1915E+08,  2.4763E+07
243   1.0000E+02,  6.2791E+08,  1.5663E+07
244   1.1000E+02,  5.0590E+08,  1.0628E+07
245   1.2000E+02,  4.1534E+08,  8.1466E+06
246   1.4000E+02,  2.8879E+08,  5.1594E+06
247   1.6000E+02,  2.0896E+08,  3.3143E+06
248   1.8000E+02,  1.5621E+08,  2.2258E+06
249   2.0000E+02,  1.1993E+08,  1.5600E+06
```

```
  2.2000E+02,  9.3814E+07,  1.1385E+06
  2.5000E+02,  6.7186E+07,  7.4414E+05
  2.8000E+02,  4.9165E+07,  5.0590E+05
  3.2000E+02,  3.3986E+07,  3.0472E+05
  3.5000E+02,  2.6526E+07,  2.1683E+05
  4.0000E+02,  1.8336E+07,  1.3287E+05
  4.5000E+02,  1.3239E+07,  8.4433E+04
  5.0000E+02,  9.8930E+06,  4.9413E+04
'End of File'
```

Listing 6: Dose in silicon as a function of aluminum shielding thickness of a sphere.

```
'*',    25,     1,     11,     10,     2,     2,     23,     0
'SPENVIS 4.6.10.3386 ---------- 23-Jul-2020 00:09:00'
'PRJ_DEF', -1,'TEST_PROJECT'
'PRJ_HDR', -1,'My Test Project'
'MOD_ABB', -1,'SH2'
'MIS_PLA',  1,    -3,' '
'MIS_NTR',  1,     1,' '
'MIS_STA',  1,  9862.00000000,' '
'MIS_END',  1, 15337.00000000,' '
'MIS_DUR',  1, 5.475000E+03,'days'
'PLT_TYP', -1,'SUMMARY'
'PLT_HDR', -1,'4pi Dose at Centre of Al Spheres'
'PLT_LEG', -1,'Solar Protons'
'PS Annotation',  8,  1
'Mission start: 01/01/1977 00:00:00'
 0.05, 0.00, 0.00
'Mission end: 29/12/1991 00:00:00'
 0.95, 0.00, 1.00
'Nr. of segments:    1'
 0.05, 1.50, 0.00
'Duration: 5475.00 days'
 0.95, 0.00, 1.00
'PS Annotation',  0,  0
'Thick','mm',  1,'Aluminium Absorber Thickness'
'Dose','rad',  1,'Dose in Si'
 1.0000E-02, 3.3911E+05
 3.0000E-02, 1.4785E+05
 5.0000E-02, 1.0308E+05
 1.0000E-01, 6.4313E+04
 2.0000E-01, 4.0112E+04
 3.0000E-01, 3.0030E+04
 4.0000E-01, 2.3338E+04
 5.0000E-01, 1.8449E+04
 6.0000E-01, 1.5023E+04
 8.0000E-01, 1.1070E+04
 1.0000E+00, 8.8504E+03
 2.5000E+00, 3.7988E+03
 5.0000E+00, 1.9959E+03
 1.0000E+01, 8.8531E+02
 1.2000E+01, 7.0294E+02
 1.4000E+01, 5.5720E+02
 1.6000E+01, 4.5273E+02
 1.8000E+01, 3.7664E+02
 2.0000E+01, 3.1782E+02
 3.0000E+01, 1.4978E+02
```

```
 5.0000E+01,  5.9685E+01
 7.5000E+01,  2.9417E+01
 1.0000E+02,  1.7294E+01
'End of File'
```

Listing 7: Dose in silicon as a function of aluminum shielding thickness of a slab.

```
'*',     25,      1,     11,     10,      2,      2,     23,      0
'SPENVIS 4.6.10.3386 ---------- 23-Jul-2020 00:12:47'
'PRJ_DEF', -1,'TEST_PROJECT'
'PRJ_HDR', -1,'My Test Project'
'MOD_ABB', -1,'SH2'
'MIS_PLA',  1,     -3,' '
'MIS_NTR',  1,      1,' '
'MIS_STA',  1,   9862.00000000,' '
'MIS_END',  1,  15337.00000000,' '
'MIS_DUR',  1, 5.475000E+03,'days'
'PLT_TYP', -1,'SUMMARY'
'PLT_HDR', -1,'Dose at Transmission Surface of Al Slab Shields'
'PLT_LEG', -1,'Solar Protons'
'PS Annotation',  8,  1
'Mission start: 01/01/1977 00:00:00'
 0.05, 0.00, 0.00
'Mission end: 29/12/1991 00:00:00'
 0.95, 0.00, 1.00
'Nr. of segments:   1'
 0.05, 1.50, 0.00
'Duration: 5475.00 days'
 0.95, 0.00, 1.00
'PS Annotation',  0,  0
'Thick','mm',  1,'Aluminium Absorber Thickness'
'Dose','rad',  1,'Dose in Si'
 1.0000E-02, 9.7044E+04
 3.0000E-02, 4.3388E+04
 5.0000E-02, 3.0446E+04
 1.0000E-01, 1.8643E+04
 2.0000E-01, 1.0959E+04
 3.0000E-01, 7.6311E+03
 4.0000E-01, 5.6987E+03
 5.0000E-01, 4.5062E+03
 6.0000E-01, 3.7338E+03
 8.0000E-01, 2.8126E+03
 1.0000E+00, 2.2703E+03
 2.5000E+00, 9.5753E+02
 5.0000E+00, 4.5323E+02
 1.0000E+01, 1.7843E+02
 1.2000E+01, 1.3491E+02
 1.4000E+01, 1.0461E+02
 1.6000E+01, 8.3682E+01
 1.8000E+01, 6.8164E+01
 2.0000E+01, 5.6500E+01
 3.0000E+01, 2.6389E+01
 5.0000E+01, 1.0762E+01
 7.5000E+01, 5.1030E+00
 1.0000E+02, 2.9528E+00
'End of File'
```

References

Donabedian, M., and D. G. Gilmore, *Spacecraft thermal control handbook*, Aerospace Press, 2003.

Joven, R., Characterization and modeling of shear stress during manufacturing and thermal properties of structural composite materials, Ph.D. thesis, Wichita State University, 2013.

Seltzer, S. M., Conversion of depth-dose distributions from slab to spherical geometries for space-shielding applications, *IEEE Transactions on Nuclear Science*, *33*(6), 1292–1297, 1986.

Ziegler, J. F., J. P. Biersack, and M. D. Ziegler, *SRIM–The stopping and range of ions in matter (2008)*, SRIM Co, 2009.